Hole Scavenging and Photo-Stimulated Recombination of Electron−Hole Pairs in Aqueous TiO_2 Nanoparticles

Ilya A. Shkrob* and Myran C. Sauer, Jr.

Chemistry Division, Argonne National Laboratory, Argonne, Illinois 60439

Received: May 25, 2004; In Final Form: June 14, 2004

It is shown that 532 and 1064 nm laser photoexcitation of trapped electrons generated by 355 nm photolysis of aqueous titania (TiO_2) nanoparticles causes rapid photobleaching of their absorbance band in the visible and near-IR. This photobleaching occurs within the duration of the laser pulse (3 ns fwhm); it is caused by photoinduced electron detrapping followed by rapid recombination of the resulting free electron and a trapped hole. The quantum yield for the electron photobleaching is ca. 0.28 for 532 nm and ca. 0.024 for 1064 nm photoexcitation. Complete separation of the spectral contributions from trapped electron and hole is demonstrated using glycerol as a selective hole scavenger. When glycerol is added to the solution, some light-absorbing holes are scavenged promptly within the duration of the 355 nm photoexcitation pulse, some are scavenged at a slower rate over the first 200 ns after the 355 nm pulse, and the rest are not scavenged, even at high concentration of the scavenger (>10 vol. %). A reaction with chemi- and physisorbed glycerol would account for the prompt and the slow hole decay, respectively. The implications of these results are discussed.

1. Introduction

Semiconducting metal oxide nanoparticles, such as aqueous TiO_2 nanoparticles, find numerous applications in photovoltaics and photocatalysis.[1−3] Photoexcitation of these nanoparticles in the UV yields electron−hole pairs that rapidly recombine; this recombination competes with trapping of the free charges by coordination defects at the surface and by lattice defects in the nanoparticle bulk. Most of these electrons and holes recombine within the first few tens of picoseconds after the photoexcitation event,[4−6] but some rapidly (<200 fs)[4] descend into traps, yielding localized species that decay slowly by bimolecular and geminate recombination on a time scale of 10^{-9}−10^{-1} s. [4−12] In the low charge density regime, the time profile of this decay exhibits dispersive $t^{-1/2}$ kinetics typical of trap-to-trap hopping observed for other disordered systems.[12,13] Most of the dynamic and structural studies of "electrons" and "holes" in titania nanoparticles are done on these *trapped* species. Though the trapped charges participate in photocatalysis, they are less reactive than their rapidly migrating, energetic precursors. For this reason, photocatalytic reactions that involve molecules in the solution are relatively inefficient,[1,2] as only trapped charges can react with such molecules. On the other hand, photooxidation and photoreduction of molecules that are chemisorbed on the nanoparticle surface can be very rapid and efficient (see, for example, refs 2, 4, 10, and 14), as these processes are due to reaction with the free carriers.

The predominant trapped-electron centers are interior and surface Ti^{III} centers that yield, respectively, narrow symmetric and broad asymmetric lines in electron paramagnetic resonance (EPR) spectra from UV-irradiated frozen solutions of TiO_2 nanoparticles at 4−77 K.[3,15−18] The structure of the hole center(s) has not yet been definitively established. The holes are trapped mainly at the surface of the TiO_2 nanoparticle and, consequently, their EPR spectra depend strongly on the surface treatment. All of these centers seem to be O 2p radicals, such as Ti^{IV}−$O^{\bullet}$ radical and adsorbed hydroxyl, $HO^{\bullet}_{ads}$.[3,15−17] According to Ishibashi et al.,[19] the quantum yield of the latter species is relatively small (ca. 0.7% of the quantum yield for the iodide-oxidizing mobile hole, see below), however, this radical is more reactive toward certain substrates. Gao et al.[20] demonstrated that only $HO^{\bullet}_{ads}$ can oxidize aliphatic monohydroxy alcohols (such as methanol) in aqueous TiO_2 nanoparticle solutions, whereas the predominant type of the hole in photoexcited TiO_2 does not react with these alcohols on the microsecond time scale.[21] Interestingly, rapid reaction of holes with alcohols was observed for clean TiO_2 surfaces exposed to alcohols, both as liquid and vapor, by time-resolved GHz conductivity[22] and IR spectroscopy.[23,24] These results, as well as EPR studies of Micic et al.,[18] suggest that the holes are scavenged by alkoxy groups anchored at the surface.[24,25] Hydrolysis of these groups by water drastically reduces hole scavenging efficiency.

Surprisingly little has been done to ascertain light absorption properties of these electrons and holes since the initial transient absorbance (TA) studies carried out in the early 1980s.[6−11] At pH = 3−4, the absorption spectrum of photoexcited TiO_2 nanoparticles is an asymmetric broad band with a maximum at 600−650 nm that extends to the IR.[6] In acidic or alkaline solutions containing hole scavengers (e.g., poly(vinyl alcohol)),[7−10] it is a broader, more symmetric band centered at 900−1000 nm.[26] A very similar band was observed by (i) electrochemical reduction of TiO_2 nanocrystalline films (at any pH and salinity of the solution in contact with the film),[27] (ii) by injection of radiolytically generated hydrated electrons into TiO_2 nanoparticles in pH = 3 solutions, [28] and (iii) in steady-state UV photolysis of the solutions containing a hole scavenger (typically, an alcohol [7−11,23] or carboxylic acid [29]). From these convergent results, it appears that the 900 nm band is from the relatively long-lived trapped *electrons*. However, it remains

* Corresponding author. Tel 630-252-9516, FAX 630-2524993, e-mail: shkrob@anl.gov.

10.1021/jp047736t CCC: $27.50
Published on Web 07/24/2004

unexplained why the TA spectra observed from photoexcited TiO_2 nanoparticles look different from this characteristic 900 nm spectrum.

Recently, TA spectra of photoexcited bare TiO_2 nanoparticles and nanocrystalline films in the 400−700 nm region became available on the femtosecond time scales, by using pump−probe ultrafast laser spectroscopy.[4,5,30,31] Though no two such TA spectra look alike (as there is considerable variation with the particle size, surface treatment, etc.), all of these spectra exhibit considerable evolution over the first few tens of picoseconds and change little afterward, suggesting that the descent to deeper traps and equilibration of the electrons and holes between different traps is largely over in 1−10 ps. The spectral features observed on nanosecond to millisecond time scales are fully developed by that delay time.[4,6]

Most workers, following the original suggestion by Rothenberger et al.[6] and Henglein,[7] assumed that the 400−1000 nm absorbance from photoexcited TiO_2 nanoparticles originated from trapped *electrons* exclusively. Such a rationale implies that more than one species of light-absorbing trapped "electrons" (i.e., Ti^{III} centers) contributes to the TA spectra: one kind of traps yields the 900 nm centered spectrum, another kind yields the 650 nm centered spectrum. In this work, we demonstrate selective removal of a subset of light-absorbing species in acidic solutions of photoexcited TiO_2 nanoparticles by using glycerol as a scavenger. We present several lines of evidence suggesting that a trapped *hole* rather than the "electron" is the progenitor of the 650 nm band. The absorption spectrum of the hole in the visible resembles the spectrum of oxidizing species in "platinized" TiO_2 nanoparticles observed by Bahnemann et al.[8−10] and tentative "trapped holes" in photoexcited TiO_2 nanocrystalline films studied by Yoshihara et al.[23] Our study suggests that the (trapped) electron in photoexcited TiO_2 nanoparticles has the same spectrum as the electron obtained by radiolytic (e.g., ref 28) and electrochemical (e.g., ref 27) reduction of TiO_2 nanoparticles and nanocrystalline films. Photoexcitation of this electron at 532 and 1064 nm causes its detrapping followed by rapid recombination with the hole. Scavenging of the hole by glycerol reduces the quantum yield of this photostimulated recombination to the same degree that it reduces the absorption of the hole. To save space, Figures 1S to 7S are placed in the Supporting Information.

2. Experimental Section

Transient absorbance was observed following 355 nm laser photoexcitation of N_2-saturated 2.4×10^{-4} M aqueous solution of 4.6 ± 0.5 nm diameter anatase nanoparticles (1400 units of TiO_2 per particle) at pH = 4. This solution was prepared and characterized as described in ref 32. The sample contained 45 ppm of aluminum by volume (that would be equivalent to 7 atoms per particle if Al^{III} were incorporated into the TiO_2 nanoparticle), and it is possible that vis-absorbing holes observed in this study originated from a $Ti^{IV}-O-Al^{III}$ or some other impurity center (section 4.3). All other chemicals were obtained in their purest form available from Aldrich and used as received.

The excitation pulse L1 (355 nm, 3 ns fwhm, 8 mJ) that was used to induce charge separation in TiO_2 was derived from the third harmonic of a Nd:YAG laser (Quantel Brilliant). The second excitation pulse (L2) of 532 nm (6 ns fwhm, 10−50 mJ) and 1064 nm light (6 ns fwhm, 90 mJ) used to photoexcite trapped electrons in TiO_2 was derived from the second and the first harmonic, respectively, of another Nd:YAG laser (Continuum model 8010). This electron-excitation pulse was delayed in time relative to the 355 nm pulse; the time jitter between these pulses was <3 ns.

The analyzing light from a superpulsed 70 W Xe arc lamp was filtered and then crossed at 45° with the 355 nm laser beam inside a 1.35 mm optical path flow cell with Suprasil windows (a 5.6 mm diameter aperture was used for light masking). The duration of the analyzing light pulse was 300 μs. The optical density (OD) of the solution at 355 nm was 0.8. The 532 nm (or 1064 nm) beam was crossed with the 335 nm beam at 25°, so that the analyzing light, the UV beam, and the 532 (1064) nm beams made the angles of 31°, −14°, and +11° with the normal to the cell window, respectively.

The transmitted light was passed through an appropriate glass cutoff filter placed before the sample, focused, passed through the sample, and then passed through another appropriate cutoff glass filter and a grating monochromator (SPEX Minimate; 450 to 950 nm). For detection at wavelengths $\lambda > 1$ μm, the analyzing light was passed through a 4 cm optical path water filter or a 400−700 nm band-pass dielectric filter to reduce the heat transfer to the sample. For detection at 1.0−1.35 μm, a set of narrow band (10 nm fwhm) interference filters at increments of 50 nm was used. The cutoff of 1.35 μm was due to the strong IR absorbance of water. For detection near 1 μm, a 0° dielectric mirror reflecting at 1064 nm was inserted before the detector to reduce the leakage of the first Nd:YAG harmonic. A fast Si photodiode (EG&G model FND-100Q) biased at −90 V was used to detect the TA for $\lambda \leq 1.1$ μm. For detection at $\lambda \geq 1.1$ μm, a fast Ge photodiode (Germanium Power model GMP-566) biased at −10 V or an InGaAs photodiode (Germanium Power model GAP-520) biased at −5 V was used. The latter photodiode is fast, but its temporal response is strongly wavelength dependent.[33] The Ge photodiode has a spectrally flat temporal response;[33] however, it is slower than the other two photodiodes, and TA kinetics acquired at delay time $t <$ 30 ns were distorted. Furthermore, a thermal lensing effect induced by the absorption of 355 nm pulse unevenly refracted the IR light across the sample causing a parasitic transient that lived for the first 20 ns after the UV photoexcitation. Thus, our near-IR spectra were not trustworthy at these short delay times.

The photodiode signal was amplified 10 times using a Comlinear model CLC449 1.2 GHz opamp and sampled using a Tektronix TD360 digital oscilloscope or a Tektronix DSA-601 digital signal analyzer. Absorption signals as small as 10^{-4} can be studied with this setup. Light emission from the sample induced by the 355, 532, and 1064 nm laser light alone was subtracted from the absorbance signal. In the following, 355 nm light induced TA kinetics are denoted $\Delta OD_\lambda(t)$, transient absorbance induced by both 355 nm (L1) and 532 or 1064 nm (L2) light is denoted $\Delta OD_\lambda^{L2}(t_{21};t)$, where t_{21} is the delay time between the laser pulses L2 and L1, and

$$\Delta\Delta OD_\lambda(t_{21};t) = \Delta OD_\lambda^{L2}(t_{21};t) - \Delta OD_\lambda(t) \qquad (1)$$

is the difference trace.

The two-pulse experiment was complicated by laser-induced precipitation of TiO_2 nanoparticles: Regardless of the flow rate of the solution, prolonged 355 nm laser irradiation caused the deposition of a thin, transparent film of TiO_2 particles on the cell windows, due to the action of a shock wave generated by the 355 nm laser. This deposit can be removed by boiling the Suprasil windows in concentrated HNO_3 for 2−3 h. Though this deposit had no discernible effect on the TA kinetics observed after the 355 nm pulse, a strong, persistent TA signal in the visible was observed when this deposit was photoexcited by 532 nm light 10−100 ns after the 355 nm pulse. For this reason, the exposure of the cell windows was limited to <1000 pulses and the cell was periodically filled with pure water to

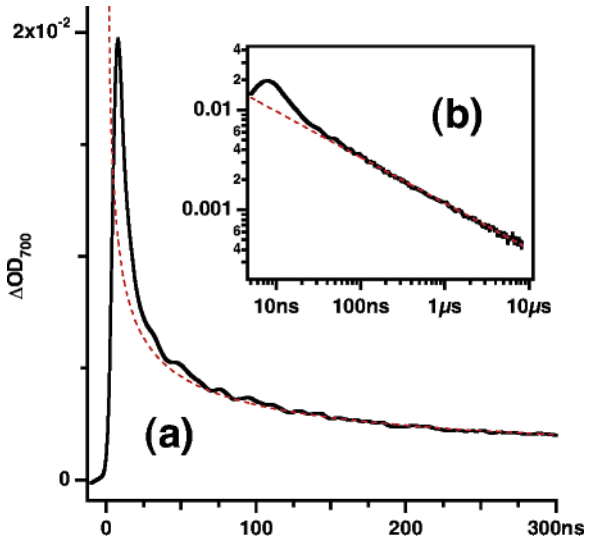

Figure 1. Solid lines: Typical decay kinetics of transient absorbance (TA) detected at $\lambda = 700$ nm following 355 nm photoexcitation of TiO_2 nanoparticles in N_2-saturated water (incident photon fluence of 64 mJ/cm^2; 24% transmission of 355 nm light). Under these photoexcitation conditions ca. 1−2 pairs are generated per nanoparticle. In (a), the first 300 ns of these kinetics are shown on a linear scale; in (b), the kinetics is shown on the double logarithmic scale. Time profiles of TA kinetics for other wavelengths of the analyzing light are shown in Figures 1S and 2S in the Supporting Information.

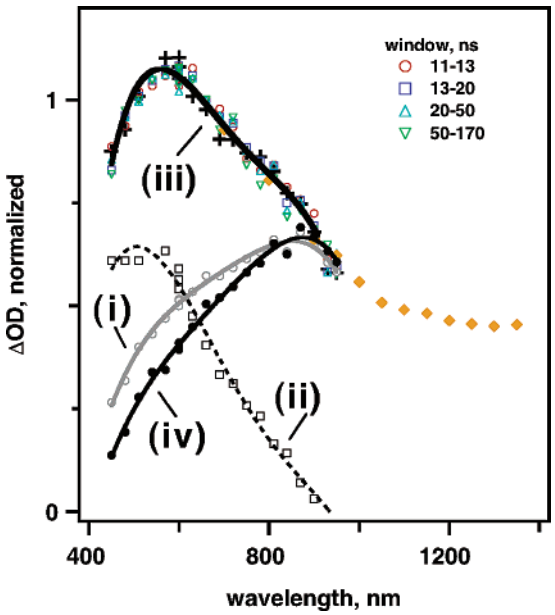

Figure 2. Open symbols: Normalized TA spectra from photoexcited TiO_2 nanoparticles. The integration windows are indicated in the legend. Filled diamonds: near-IR spectrum from the same photosystem (50−200 ns integration). The TA spectra in the near-IR also do not depend on the delay time (see Figure 2S). Traces (i) to (iii) demonstrate the decomposition of the TA spectrum into the contributions from trapped electrons and holes. Trace (i) is the normalized TA spectrum at 200−370 ns from TiO_2 nanoparticle solution containing 5 vol. % glycerol. Trace (ii) is the normalized spectrum of the light-absorbing holes (see Figure 5b). The sum of these two absorptions gives trace (iii) (crosses). Trace (iv) gives the electron absorbance only (see Figure 8b). The solid lines are guides for the eye.

monitor for the formation of the film deposit. For the same reason, a cell with detachable optical windows has been used. The typical flow rate was 0.5−2 cm^3/min and the repetition rate of the laser was 1−2 Hz.

In some experiments, a hole scavenger (1−5 vol. % glycerol) was added to the reaction mixture. The C-centered (-olyl) radicals generated in the photooxidation of glycerol by holes in the TiO_2 nanoparticles do not absorb light at $\lambda > 400$ nm. To prevent the buildup of a permanent trapped-electron absorbance during continuous laser photolysis, the sample was saturated with O_2. The oxygen reacts with the electrons on a millisecond time scale,[34] making the photosystem reversible. Control experiments with N_2-saturated TiO_2 nanoparticle solutions showed that the oxygen does not react with the electrons on the time scale of our study (<10 μs, Figures 1S and 2S). In another control experiment, an N_2-saturated, glycerol-containing solution of TiO_2 nanoparticles was continuously illuminated with 300−400 nm light from the Xe arc lamp for 1 h to induce a strong absorbance from the trapped electrons (the OD of this solution at 400−900 nm was 0.07−0.1) and then TA kinetics were obtained following the 532 nm laser photoexcitation. No 532 nm light induced transient photobleaching was observed, nor did we observe any photobleaching when the UV-photolyzed N_2-saturated glycerol solution was illuminated with 1−5 mW of visible light for 1−2 h.

Since under the conditions of our TA experiment < 1−2 electron−hole pairs per particle were present at the end of the 355 nm pulse,[25] scavenging of the hole by glycerol results in a long-lived TA signal from electrons which lack hole partners on the same nanoparticle (referred to as the "persistent" electron in the following).

3. Results

3.1. Single Pulse 355 nm Photoexcitation. Figure 1 shows typical TA kinetics observed in 355 nm laser photolysis of aqueous TiO_2 nanoparticles ($\lambda = 700$ nm). The initial "spike", whose time profile closely follows the temporal response function of the setup (Figure 1a), is rapidly succeeded by the power law $t^{-\alpha}$ decay with $\alpha \approx 0.46$ (Figure 1b). This slow decay kinetics can be followed out to at least 100 μs. Exactly the same time profiles of transient absorbance are observed across the entire visible, for $t > 5$ ns (Figure 1S), and in the near-IR, for $t > 20$ ns (Figure 2S). Since all of these time profiles are identical, there is no time evolution of the TA spectrum. In Figure 2, normalized TA spectra in the visible obtained at different delay times are plotted together (Figure 3a shows the typical evolution of the TA spectra prior to the normalization). All of these spectra are identical within the experimental scatter (see also Figure 4a). As seen from Figure 2S, the same applies to the TA spectra obtained in the near-IR (filled diamonds in Figure 2). For $\lambda > 900$ nm, minor changes in the spectrum were observed within the first 20 ns. These changes turned out to be a combined effect of the slow photoresponse of the Ge photodiode[33] and wavelength-dependent refraction of the analyzing light by a thermal lens in the sample (section 2).

Qualitatively similar TA spectra (400−900 nm) and TA kinetics (<1 μs) were observed for TiO_2 nanoparticles in acidic solutions by previous workers.[7−10] Unlike some of these workers (see, for example, Rothenberger et al.,[6] Bahneman et al.,[10] Yoshihara et al.[23]) we found no evidence of time evolution for TA spectra over the first 10 μs after the photoexcitation, both in N_2- and O_2-saturated solutions. In particular, no effect of oxygen was observed.[10,23] In this respect, our study is in agreement with the recent pulse radiolysis study of Gao et al.[34] reporting the kinetics for a reaction between the O_2 and radiolytically generated electrons on 4.7 nm diameter aqueous titania nanoparticles. Scavenging constants of 10^4−10^5 M^{-1} s^{-1} were obtained from a multiexponential fit of the dispersive kinetics. Given that the concentration of oxygen in the saturated solution is ca. 10^{-3} M, electron scavenging by O_2 is too slow

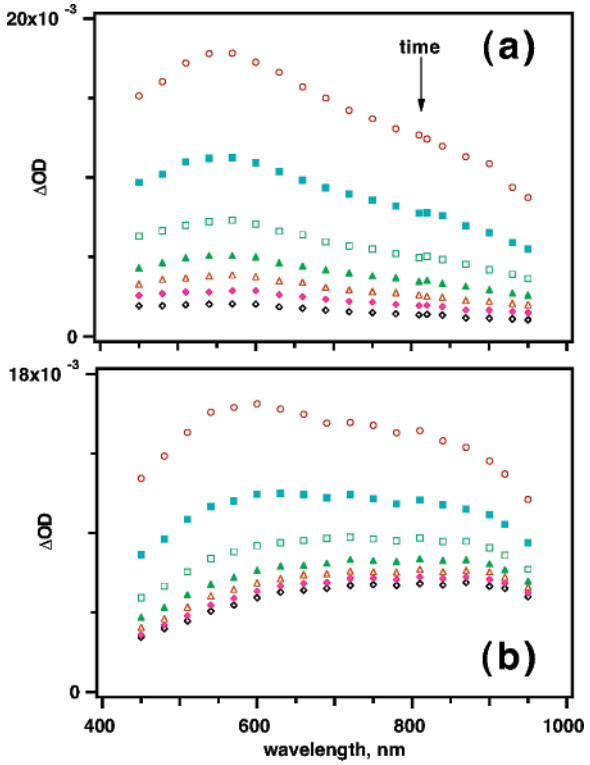

Figure 3. Time evolution of TA spectra (400−1000 nm) obtained under identical photoexcitation conditions in oxygen saturated (a) aqueous solution of TiO_2 nanoparticles and (b) the same solution containing 5 vol. % of glycerol. The integration windows are, from top to bottom, 9−13 ns (open circles), 13−23 ns (filled squares), 23−45 ns (open squares), 45−75 ns (filled triangles), 75−120 ns (open triangles), 120−200 ns (filled diamonds), and 200−370 ns (open diamonds), respectively. The time evolution of the near-IR spectrum for glycerol solution is shown in Figure 3S.

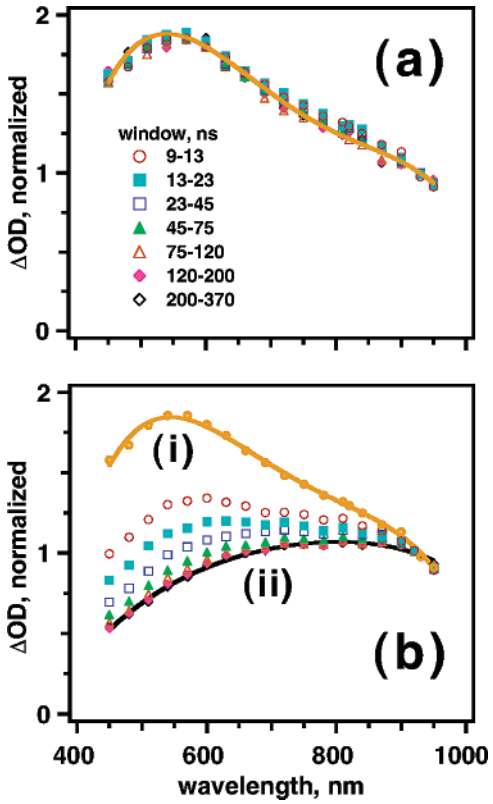

Figure 4. TA spectra from Figure 3 normalized by the absorbance signal at 900 nm (same symbols as in Figure 3; see the legend in (a)). In (b), trace (i) is the prompt TA spectrum from (a) and trace (ii) is the "final" TA spectrum attained at 200−370 ns. The solid lines are guides to the eye. See also Figure 4S, which gives the TA kinetics from the 5 vol. % glycerol solution that are normalized at 200 ns. The short-lived TA signal in the visible is from the holes.

to interfere with our kinetic measurements. Neither did we observe spectral changes when more electron affinic scavengers, such as dimethyl sulfoxide, tetranitromethane, SF_6, were added to the aqueous solution. Apparently, trapped electrons in the TiO_2 nanoparticles reacted too slowly with these neutral scavengers (the reactions with ionic scavengers, such as NO_2^- and ClO_2^- are notably faster).[34] Yet the reaction eventually occurred since addition of these scavengers prevented the development of permanent blue coloration from the trapped electron in the presence of hydroxylic hole scavengers. We stress that the signal-to-noise ratio in our TA kinetic traces was better than in the previous experiments, and we are confident that if there were a spectral evolution similar to that observed in refs 6 and 10, it would be observed using our TA setup.

As mentioned above, most researchers attribute the spectrum shown in Figure 2, trace (iii), to trapped electrons, though some studies suggested that trapped holes may also absorb in the visible (section 4.3). Our results suggest that the TA spectrum shown in Figure 2 is a composite spectrum of the absorbances from the electron and the hole. The resulting TA spectrum can be decomposed into the individual components by addition of a suitable hole scavenger, as discussed below.

Addition of 5 vol. % of hole scavenger, glycerol, to oxygenated solution of TiO_2 nanoparticles (see section 2) strongly reduces the TA signal in the visible and simultaneously increases the TA signal in the near-IR, as shown in Figure 3b (compare with the TA spectra in Figure 3a obtained under the same excitation conditions and time windows for an O_2-saturated solution without the hole scavenger). Even the prompt TA spectrum obtained at the end of the 3 ns fwhm, 355 nm pulse is quite different from the TA spectrum shown in Figure 3a. Further evolution occurs within the first 200 ns after the 355 nm photoexcitation pulse; at later delay times the TA spectrum stops changing (Figure 3b). Importantly, the addition of the hole scavenger has almost no effect on the shape of the TA spectrum for $\lambda > 900$ nm. This point can be demonstrated by comparing the TA spectra obtained at different delay times at 900−1300 nm, as shown in Figure 3S. In Figures 4a and 4b, the TA spectra shown in Figure 3 were normalized at 900 nm. Without glycerol, all the normalized spectra are the same. For the glycerol solution, a spectral component in the visible is missing from the onset. At later delay times, more of this component is missing, as the species which absorbs light in the visible decays on a sub-microsecond time scale. This point is illustrated in Figure 4S, where 450−950 nm TA kinetics in 5 vol. % glycerol solution are normalized at 200 ns (by which delay time the spectral evolution is over). These normalized kinetics diverge in the first 50 ns after the photoexcitation, suggesting rapid spectral evolution on this short time scale.

To obtain the spectrum of the short-lived species, normalized TA spectra obtained at $t < 200$ ns (Figure 4b) were subtracted from the normalized spectrum obtained at $t > 200$ ns (Figure 5a, trace (ii)). As shown in Figure 5b, the resulting difference traces do not change in shape with the delay time, which implies that the missing spectral component (trace (i) in Figure 5b) originates from a *single* light-absorbing species. Eventually (at $t > 200$ ns), all of this species decays and the spectrum shown by trace (ii) in Figures 5a and 5b is obtained. This "final" TA spectrum does not depend on the glycerol concentration (1 to 10 vol. %). Since -olyl radicals derived from glycerol do not

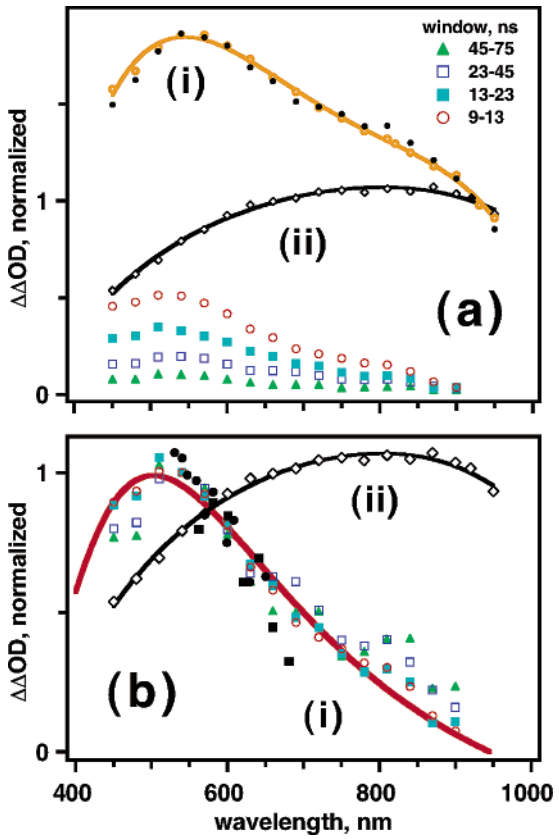

Figure 5. (a) Symbols: difference TA spectra (same coding as in Figure 4) obtained by subtraction of the TA spectrum at 200−370 ns from other traces (excepting curve (i)) in Figure 4b (5 vol. % glycerol solution). The spectrum at 200−370 ns (open diamonds) is shown by trace (ii); trace (i) (open circles) is the same as trace (i) in Figure 4b. The solid lines are guides to the eye. Filled circles give a weighted sum of trace (ii) and the prompt TA spectrum of the hole (open circles). (b) Same as (a); the difference spectra were normalized to illustrate that the spectrum of the species that is "removed" by glycerol over the first 200 ns after 355 nm photoexcitation does not change with the delay time (trace (i)). For comparison, trace (ii) from (a) is reproduced. Filled symbols are normalized TA spectra of (tentative) vis-absorbing holes: filled circles are from ref 8 (Figure 8 therein), filled squares are from ref 10 (Figure 5 therein).

absorb in the visible, this final spectrum is mainly from a trapped electron (though, as shown below, a small fraction of holes also contribute to the long-lived TA signal).

Spectra from trapped electrons similar to the TA spectrum shown by trace (ii) in Figure 5b have been observed by other researchers, in particular, (i) in laser photolysis of basic solutions of TiO_2 nanoparticles,[26] (ii) in steady-state UV photolysis (e.g., refs 7, 26, and 29) and pulse radiolysis[28] of acidic TiO_2 solutions, and (iii) by spectrophotometry of electrochemically reduced thin TiO_2 films in contact with basic or acidic solutions. [27] In all of these experiments, the trapped holes either were not generated or were promptly scavenged after their generation. Apparently, it is the presence of the hole on the aqueous TiO_2 nanoparticle that is responsible for the difference in the TA spectra shown in Figures 3a and 3b. The difference traces shown in Figure 5a thereby give the absorption spectrum of the hole (trace (i) in Figures 2 and 5b). These spectra, with peak absorbances at ca. 480 nm and gradual decrease in absorbance toward the near-IR, strikingly resemble the absorption spectra of the tentative hole species obtained by Bahnemann et al.[8−10] by photoexcitation of "platinized" TiO_2 nanoparticles and by Yoshihara et al.[23] by photoexcitation of methanol-wetted TiO_2 nanocrystalline films (section 4.3). The islands of metallic Pt deposited on the nanoparticle surface serve as efficient electron traps, and Bahnemann et al.[8−10] attribute the TA spectra observed from the "platinized" TiO_2 nanoparticles to holes.

Importantly, a weighted sum of the spectral contributions from the "hole" (trace (i) in Figure 5b) and the "electron" (trace (ii) in Figure 5b) shown in Figures 2 and 5a *exactly* reproduces the TA spectrum observed in the TiO_2 nanoparticle solution that does not contain glycerol (trace (i) in Figure 5a and trace (iii) in Figure 2). Thus, both of the spectral components are also present in the solution that does not contain glycerol.

The data shown in Figure 4b can be used to estimate the proportions of the hole scavenging during and after the photoexcitation pulse. The normalization at 900 nm, where the hole does not absorb, allows a determination of the decrease in the absorption in the visible caused by scavenging of the hole. The absorbances for the longest time window shown in Figure 4b are essentially all due to electrons only, because, as shown below, only 5−10% of the holes are not scavenged by 5 vol. % glycerol. Therefore, the difference between traces (i) and (ii) is a measure of the "total" scavengeable holes. For example, the difference between trace (i) and the 9−13 ns data (open circles) is a measure of the holes promptly scavenged during the 355 nm laser pulse. In this way we obtain that ca. 45−50% of the light absorbing holes are scavenged within the duration of the 355 nm photoexcitation pulse, while another 45% are scavenged over the first 200 ns after the photoexcitation (these percentages are given relative to the electron concentration present at the beginning of this reaction, Figure 4b). Since most of the holes present by the end of the 355 nm pulse decay by recombination rather than by this slow scavenging (see Figure 9 below), such a reaction contributes very little to the net yield of persistent electrons at $t > 200$ ns.

As the scavenger concentration increases (Figures 6a and 5S), the fraction Φ_e of trapped electrons observed at $\lambda \geq 900$ nm that avoid recombination with the hole and persist at $t > 300$ ns steadily increase from ca. 10% toward ca. 50% (see Figures 7a and 5S(a) and Figure 2 in ref 25). This fraction was determined by taking the ratio of the near-IR absorbance at 300−350 ns and the (maximum) prompt absorbance ΔOD_λ^{max} at the end of the 355 nm pulse. Exactly the same fractions of Φ_e were obtained at $\lambda = 900$, 1100, and 1300 nm (Figure 5S(c)), i.e., across the whole spectral range where the TA spectrum is dominated by the electron absorption. The increase in the fraction Φ_e of persistent electrons as a function of scavenger concentration follows the equation (Figures 7a and 5S(c))

$$\Phi_e \approx A + B\frac{K_h[\text{glycerol}]}{1 + K_h[\text{glycerol}]} \qquad (2)$$

with the half-effect concentration K_h^{-1} of 0.435 M (where A and B are empirical constants). Very similar behavior was observed for other polyhydroxy hole scavengers, such as carbohydrates.[25] As shown in ref 25, the constant K_h varies over several orders of magnitude, depending on the number of the anchoring HO groups. On the other hand, addition of 1−50 vol. % of monohydroxy alcohols has no effect on the TA kinetics observed in the visible (where both the hole and the electron absorb light) or near-IR (where only electrons absorb light). This result has been previously obtained by Rabani et al.,[21] and it is fully confirmed in the present work. (Note that monohydroxy alcohols rapidly (<10 ns) react with holes on dry TiO_2 surfaces exposed to neat liquid alcohols[21,23] and alcohol vapor;[24] the reaction is inefficient only in the *aqueous* solutions of these

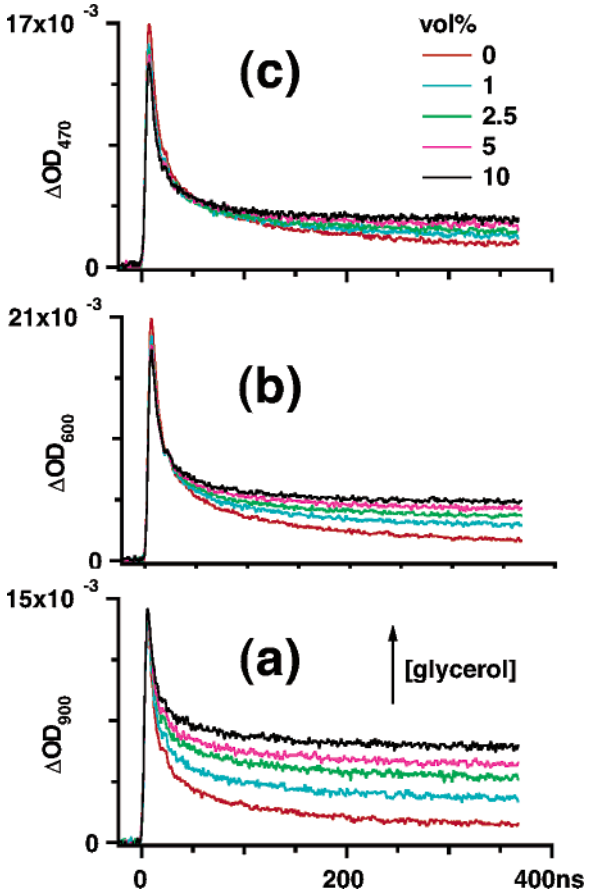

Figure 6. Decay kinetics of TA observed, using (a) 900 nm, (b) 600 nm, and (c) 470 nm analyzing light, from oxygenated aqueous TiO_2 nanoparticle solution containing 0, 1, 2.5, 5, and 10 vol. % glycerol. These kinetics were obtained under identical photoexcitation conditions using the same stock solution. Only the first 370 ns after the photoexcitation are shown. The TA kinetics at 900 nm (where only trapped electrons absorb) gives the decay kinetics of the electron.

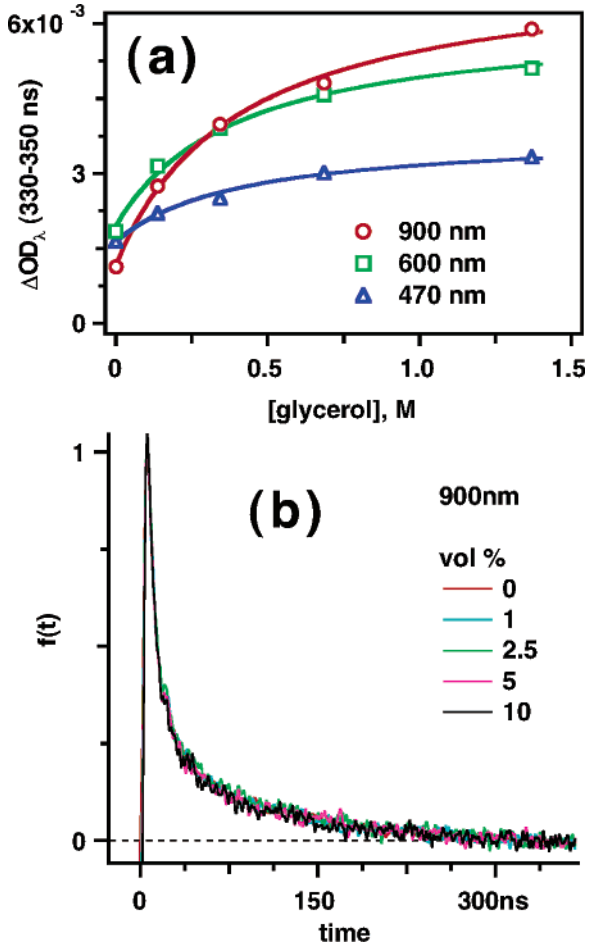

Figure 7. The data of Figure 6, replotted. (a) TA signals attained at 330−350 ns (at which time all the holes that can be scavenged by glycerol have been scavenged) vs [glycerol]. These TA signals are for $\lambda = 470$ nm (open triangles), 600 nm (open squares), and 900 nm (open circles). The solid lines are least-squares fits using eq 2; the constant K_h is the same for all three dependencies. (b) The plot of functions $f_{900}(t)$ given by eq 3 obtained from the data of Figure 6a for glycerol concentrations given in the legend. The persistence of $f_\lambda(t)$ with [glycerol] is observed for all wavelengths $\lambda \geq 900$ nm (e.g., Figure 5S).

alcohols, due to the efficient hydrolysis of alkoxy groups by the solvent.) The same negative result was obtained for acetic and malonic acid, which were commonly used as hole scavengers in previous photochemical studies. [29] Neither the TA signal from the hole decreases, nor the TA signal from the electrons increases. Apparently, hole scavenging by these compounds is slow and inefficient.

Importantly, when the plateau absorbance attained at $t > 300$ ns is subtracted from the 900−1300 nm kinetics and the resulting difference traces are normalized at the TA signal maximum, the resulting $f_\lambda(t)$ kinetics

$$f_\lambda(t) = \frac{\Delta OD_\lambda(t) - \Delta OD_\lambda(t = 330\ \text{ns})}{\Delta OD_\lambda^{\max} - \Delta OD_\lambda(t = 330\ \text{ns})} \qquad (3)$$

are identical within the experimental error. This point is illustrated in Figure 7b (for $\lambda = 900$ nm) and Figures 5S(a) and 5S(b) (for $\lambda = 1100$ nm and $\lambda = 1300$ nm, respectively). We conclude that the decay kinetics of electrons in the presence of a hole scavenger is a weighted sum of a constant and the decay kinetics obtained in the absence of the hole scavenger.

These observations suggest that there is a subset of holes that are scavenged very rapidly by the glycerol (well within the duration of the photoexcitation pulse) or, perhaps, whose generation is prevented by the presence of glycerol (if the latter reacts with their short-lived precursor).[35] Thus, in the glycerol solution, the TA signal at $\lambda \geq 900$ nm originates from two types of trapped electrons: (i) the persistent electron residing on a nanoparticle with a hole removed or transformed in a reaction with the scavenger, and (ii) relatively short-lived electron residing on the nanoparticle which still has a hole. Naturally, for the latter electrons, the decay kinetics are exactly the same as those for the electron on a TiO_2 nanoparticle in the aqueous solution.

The same effect, viz., the relative increase in the long-lived, persistent TA signal at $t > 200$ ns with the addition of a hole scavenger, was observed across the entire visible range (where both the electron and the hole absorb light); see Figures 6b, 6c, and 7a. The magnitude of this effect increases with increasing wavelength λ of the analyzing light. In Figure 7a, the concentration dependencies for ΔOD_λ at 330−350 ns for $\lambda = 470$, 600, and 900 nm are fit by the dependencies given by the left-hand side of eq 2 with the same constant K_h for all three wavelengths. This plot indicates that the reaction with glycerol trades the spectral contribution from the hole for the spectral contribution from the persistent electron which, once formed, does not decay on the microsecond time scale. The same point is demonstrated by Figure 8a, where the "final" absorbances ΔOD_{470} and ΔOD_{600} attained at $t = 330-350$ ns are plotted as a function of the "final" optical density ΔOD_{900} for several glycerol concen-

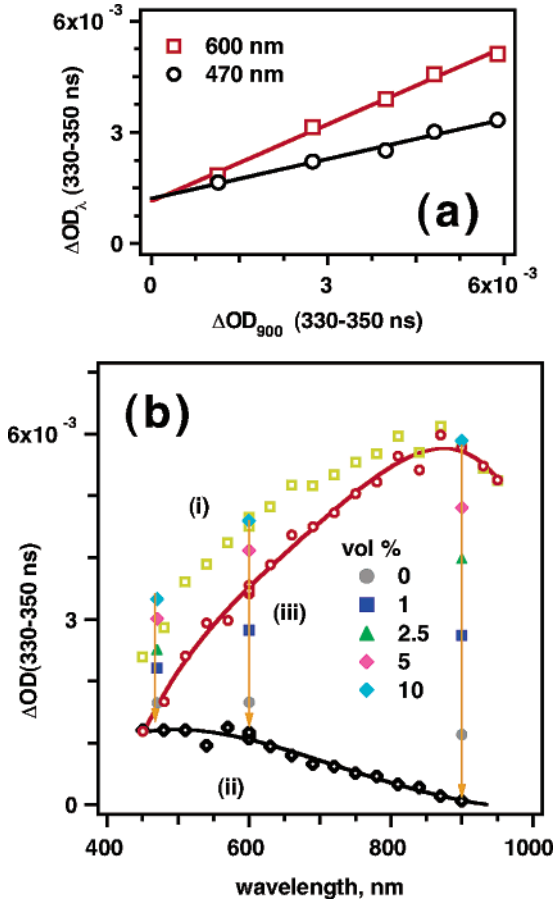

Figure 8. (a) The TA signals at $\lambda = 470$ nm (open circles) and $\lambda = 600$ nm (open squares) plotted as a function of $\lambda = 900$ nm absorbance for several glycerol concentrations. The higher absorbances correspond to the higher glycerol concentration. These dependencies are linear, suggesting that addition of glycerol increases the TA signals in the visible (attained when the hole scavenging is complete) in the same proportion as it increases the electron absorbance at 900 nm. (b) The "reconstruction" of the residual spectrum. Filled symbols show the TA signals at 470, 600, and 900 nm (at $t > 200$ ns) as a function of glycerol concentration. The vertical arrows point to the "residual absorbances" obtained by linear extrapolation of plots in (a). Trace (i) (open squares) is the TA signal attained at 330−350 ns in 10 vol. % glycerol solutions (which does not change in shape as a function of [glycerol]). Trace (ii) is a scaled absorption spectrum of the hole reproduced from Figure 2, trace (ii). The arrows at 600 and 470 nm point to this spectrum. The same is observed at other wavelengths in the visible (not shown). When this "residual" absorbance is subtracted from trace (i), the difference trace (iii) gives the absorption spectrum of the electron.

trations. These plots are linear. The intercepts of these plots correspond to the 470 and 600 nm absorbances that originate from the holes that cannot be scavenged by glycerol (i.e., whose absorbances cannot be traded for the electron absorbance) even when a large concentration of glycerol is added to the reaction mixture. The TA signals from these "unscavengeable" holes are shown in Figure 8b (with the arrows pointing to the corresponding values). Traces (i) and (ii) in Figure 8b are normalized spectra of the "electron" and the hole given by traces (i) and (ii) in Figure 2, respectively. Apparently, this "electron" spectrum is, in fact, composite, because some light-absorbing holes are not scavenged by glycerol on the microsecond time scale. The "scavengeable" (>90%) and "unscavengeable" (<10%) holes have similar TA spectra. Assuming that these absorption spectra are identical, the residual hole spectrum trace (ii) can be subtracted from the "final" spectrum, trace (i), in the same figure. This procedure gives a bell-shaped spectrum of the trapped electron alone (trace (iii) in Figure 8b). The same

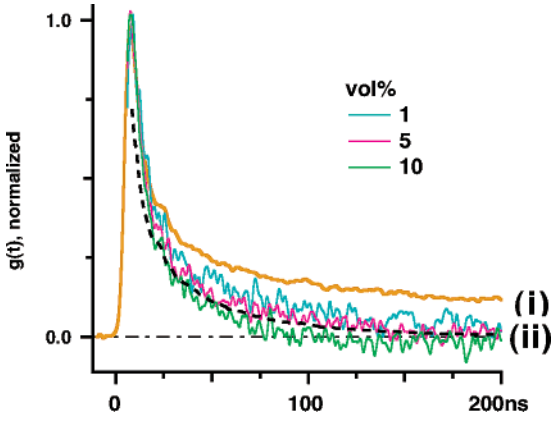

Figure 9. Thin solid lines: Normalized decay kinetics for the visabsorbing, "scavengeable" holes (functions $g_{600}(t)$ given by eq 4) at three concentrations of glycerol (1, 5, and 10 vol. %, as indicated in the color scale). Trace (i) (bold line) is the normalized decay kinetics of the electron in aqueous solution with no glycerol, obtained at 900 nm (which must be the same as that of the hole in such a solution). Trace (ii) (dashed line) is trace (i) weighted by $\exp(-t/\tau_h)$ with $\tau_h \approx 130$ ns.

spectrum is shown in Figure 2, trace (iv). Since any TA spectrum that is a linear combination of traces (i) and (ii) in Figure 2 is also a linear combination of traces (ii) and (iv) in the same figure, our conclusion that the TA spectrum in water (trace (iii) in Figure 2) is the composite spectrum of the electron and the hole is still correct.

As mentioned above, ca. 45−50% of the visible-light-absorbing holes are scavenged by glycerol promptly, and the remaining holes are scavenged slowly over the first 200 ns after the photoexcitation (Figure 4b). The kinetics of this slow hole-scavenging reaction can be observed by normalizing the kinetic trace obtained in the visible (where both the electron and the hole absorb, Figure 6b) and at $\lambda = 900$ nm (where only the electron absorbs, Figure 6a) by the "final" absorbance attained at $t = 330-350$ ns and then taking the difference of these two normalized traces:

$$g_\lambda(t) = \frac{\Delta OD_\lambda(t)}{\Delta OD_\lambda(t = 330\ \text{ns})} - \frac{\Delta OD_{900}(t)}{\Delta OD_{900}(t = 330\ \text{ns})} \quad (4)$$

This procedure removes the contribution to TA from the electrons and "unscavengeable" holes, i.e., the resulting traces are the decay kinetics of the "scavengeable" holes. The resulting traces are shown in Figure 9. To facilitate the comparison between these kinetics, the traces were normalized at the maximum. It is remarkable that these decay kinetics barely change as a function of glycerol concentration. Furthermore, most of this decay is due to recombination of the holes with the electrons. The recombination decay of these electrons in the absence of a scavenger (as observed at $\lambda = 900$ nm) is given by trace (i) in Figure 9; the decay kinetics of the holes (at $\lambda = 600$ nm) can be obtained by weighting these kinetics by an exponential function with a time constant τ_h of ca. 130 ns (trace (ii) in Figure 9).

The fact that this "slow" hole-scavenging reaction shows almost no dependence on the glycerol concentration suggests that this reaction does not involve a glycerol molecule in solution, as otherwise the kinetic mass law would be obeyed. Rather, it should involve a *physisorbed* glycerol molecule. Once the coverage of the nanoparticle by glycerol is total (which occurs at 0.3−0.7 vol. %), the reaction rate cannot increase further. Thus, we suggest that hole scavenging by glycerol (and

polyols, in general) is two-stage.[25] First, the holes are promptly scavenged by *chemisorbed* molecules that chelate the titanium atom at the nanoparticle surface (see ref 25 for more detail). This reaction is very rapid (taking perhaps < 10 ps);[4] it competes with charge recombination and trapping of the hole by other surface defects. Once this ultrafast reaction is over, the surviving holes (which descended to deep traps) slowly react with physisorbed polyol molecules by H-abstraction or charge transfer. The residual holes (which are a small fraction of the total) are trapped by lattice defects in the subsurface or the interior of the nanoparticle and cannot react with physi- or chemisorbed polyols (on the microsecond time scale). Previously, Bahnemann et al.[10] used nanosecond flash photolysis to study hole scavenging by thiocyanate and dichloroacetate and reached similar conclusions. Some holes react with the adsorbed hole scavengers promptly within the duration of the laser pulse (ultrafast pump−probe spectroscopy studies of Bowman et al.[4] suggest that for thiocyanate, this prompt reaction occurs on the femtosecond time scale), some holes react more slowly (at least, for dichloroacetate), and some holes do not react at all, at any concentration of the hole scavenger. While not all of our observations are in perfect agreement with the study of Bahnemann et al.[12] (e.g., we did not observe the effect of oxygen on the evolution of TA spectra), the general features of the hole dynamics observed in the present work (two-stage hole scavenging, different subspecies of these holes, the absorbance from the holes in the visible) are strikingly similar to those observed in ref 10, despite the different experimental approach and the different nature of the hole scavengers.

Since the TA spectrum shown in trace (iii) in Figure 2 is composite, an explanation is due as to why in the absence of a hole scavenger both of the species that contribute to this spectrum decay in exactly the same manner over many decades in time. This behavior is readily accounted for provided that the contributing absorbances originate from the electron and the hole, as suggested above. Indeed, if the latter species decay by recombination, there would always be a parity between their concentrations. Another piece of evidence favoring this scenario is given in the next section, which deals with photostimulated recombination of the electron−hole pairs.

3.2. 532 and 1064 nm Light Induced Photobleaching of the TA Absorbance. Figure 10a demonstrates a change in the TA kinetics induced by a short pulse of 532 light applied at delay time $t_{21} = 24$ ns following 355 nm photoexcitation ($\lambda =$ 600 nm). In this plot, trace (i) shows the decay kinetics without the 532 nm pulse, trace (ii) shows the decay kinetics with the 532 nm pulse, and trace (iii) shows the difference kinetics given by eq 1. As seen from Figure 10a, the TA signal (trace (ii)) first rapidly decreases within the duration of this 532 nm pulse, then recovers on the same time scale as the ΔOD_{600} kinetics decays. Figure 10a, trace (iv) shows the normalized difference trace (iii) (the recovery kinetics of the $\Delta\Delta OD_{600}$ signal) juxtaposed on the TA kinetics induced by the absorbance of the 355 nm light alone (trace (i)). As seen from Figure 10a, these two kinetics are identical within experimental error, and this situation persists out to at least $t = 15$ μs.

These observations suggest that the 532 nm photoexcitation promptly depletes at least one of the species that absorb 600 nm light within the duration of the 532 nm excitation pulse. However, not all of these species are photobleached; some remain in the reaction mixture well after the 532 nm photoexcitation, and these remaining species have exactly the same decay kinetics as the 600 nm light absorbing species following 355 nm photoexcitation. This conclusion pertains not only to the TA kinetics observed at $\lambda = 600$ nm but also to all TA kinetics observed between 400 and 1350 nm. Furthermore, it holds for both 532 and 1064 nm photoexcitation (Figure 6S).

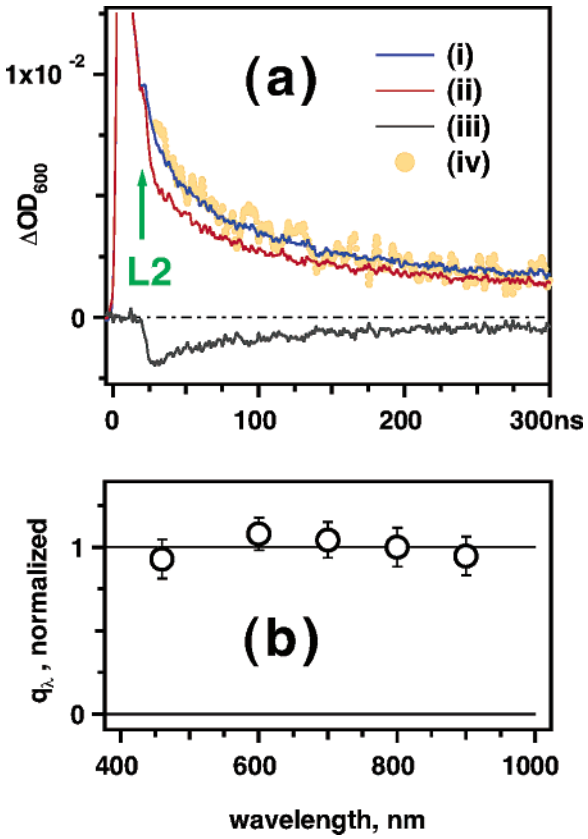

Figure 10. (a) Photobleaching of the TA signal from N_2-saturated aqueous solution of TiO_2 nanoparticles observed at $\lambda = 600$ nm. The electrons were photoexcited by a 532 nm laser (L2) pulse (6 ns fwhm, 40 mJ). The instant at which this pulse is fired, at the delay time $t_{21} =$ 24.5 ns after the 355 nm pulse (3 ns fwhm, 10 mJ), is indicated by an arrow. Trace (i) is the $\Delta OD_{600}(t)$ kinetics (no 532 nm photoexcitation). Trace (ii) is the $\Delta OD_{600}{}^{L2}(t_{21};t)$ kinetics observed following the consecutive 355 and 532 nm photoexcitations. Trace (iii) is the difference of these two traces. Trace (iv) (filled circles) is the inverted and normalized trace (iii) juxtaposed onto trace (i). (b) The fraction q_λ of the TA signal photobleached by 532 nm light (same photoexcitation conditions as in plot (a)) plotted as a function of the wavelength λ of the analyzing light. To facilitate the comparison, q_λ at 800 nm was taken to be unity.

Let us introduce the fraction q_λ of the TA signal that is promptly photobleached by the 532 nm (or 1064 nm) light, defined as the ratio

$$q_\lambda = -\Delta\Delta OD_\lambda(t_{21};t \approx t_{21})/\Delta OD_\lambda(t \approx t_{21}) \qquad (5)$$

of the photobleached TA signal to the TA signal at $t = t_{21}$. As explained above, this quantity is fully sufficient to characterize the entire photobleaching dynamics because the temporal behaviors of the $\Delta\Delta OD_\lambda(t_{12};t)$ and $\Delta OD_\lambda(t)$ kinetics are exactly the same (traces (iii) and (i) in Figure 10a, respectively). Due to this similarity, it is possible to fit both of these kinetics using the same smooth function (for instance, a biexponential dependence) and extrapolate these dependencies to $t = t_{21}$, thereby increasing the accuracy with which the quantity q_λ is estimated. The resulting photobleaching fractions q_λ obey the following simple rules, for both 532 and 1064 nm photoexcitation. For a given photon fluence of laser L2, the fraction q_λ does not depend on the observation wavelength λ (Figure 10b) or on the delay time t_{21} between the laser pulses L2 and L1.

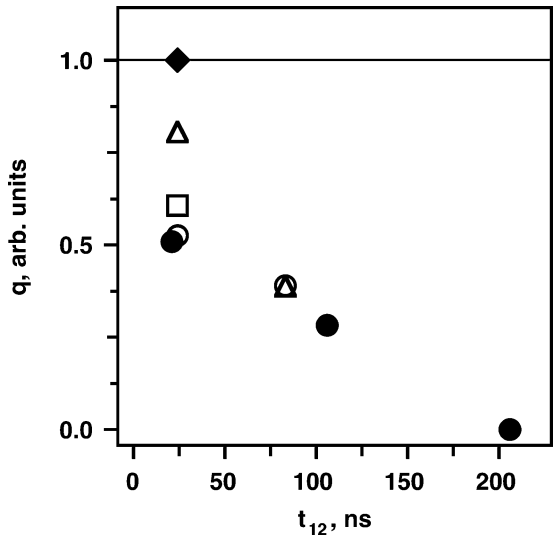

Figure 11. The photobleaching efficiency q_λ given by eq 5 for $\lambda = 600$ nm vs the delay time t_{21} between the 532 and 355 nm lasers. All data points were obtained under identical excitation conditions. The bleaching efficiency in the aqueous solution of TiO_2 nanoparticles containing no glycerol was taken for unity (filled diamonds); this quantity does not change with the delay time t_{21}. The concentrations of added glycerol, in vol. %, were 1 (open triangles), 2.5 (open squares), and 5 (open circles). Filled circles indicate the data obtained for 5 vol. % glycerol at $\lambda = 900$ nm.

This fraction linearly increases with the photon fluence of laser L2. Addition of a hole scavenger, such as glycerol, (Figure 11) causes a decrease in q_λ; this decrease becomes greater at longer delay times, t_{21}, between the laser pulses.

The linear increase in the photobleaching efficiency with increasing 532 nm (or 1064 nm) photon fluence indicates that the photoexcitation is 1-photon. The independence of the ratio q_λ on the delay time t_{21} means that a constant fraction of the 532 nm (or 1064 nm) light absorbing species is photoexcited at any time on the TA vs time curve. The lack of wavelength dependence means that the profile of the photobleaching spectrum is identical to that of the species before the 532 or 1064 nm photoexcitation. That would not be remarkable if the TA spectrum shown in Figure 2, trace (iii) originated from a single light-absorbing species depleted by the 532 or 1064 nm photoexcitation. However, as shown in the previous section, this does not seem to be the case. Thus, to account for our observations it is necessary to postulate that the 532 or 1064 nm photoexcitation of *one* of the light absorbing species depletes *both* of these species, in exactly the same ratio with which these two species were present prior to the photoexcitation. For example, as explained in section 3.1, the TA signal at 1064 nm is from trapped electrons only. If only electrons were depleted in the course of 1064 nm photoexcitation, the fractions q_λ at $\lambda = 600$ nm (where both the electron and the hole absorb) and at $\lambda = 900$ nm (where only the electron absorbs) would be different. Experimentally, these two fractions are the same within 10%. The same argument pertains to the 532 nm photoexcitation. Thus, either the spectrum shown in Figure 1, trace (iii) is from a single species (section 4.2), contrary to the arguments presented above, or exactly the same fraction of electrons and holes decays following 532 or 1064 nm photoexcitation. In the latter case, only photostimulated recombination can account for the observed behavior.

The effect of the hole scavenger on the photobleaching strengthens the latter explanation. A steady-state concentration of trapped electrons in TiO_2 nanoparticles can be generated by continuous UV illumination of N_2-saturated aqueous solution containing a hole scavenger (in our case, glycerol). After 30 min illumination by 300−400 nm light, an optical density of 0.2−1 at 532 nm from trapped electrons was obtained (in a 1 mm optical path cell). When this solution was photolyzed using 532 and 1064 nm pulses, no transient photobleaching, either temporary or permanent, was observed. This negative result suggests that in the absence of a hole localized on the same TiO_2 nanoparticle, laser excitation of trapped electron does not lead to photobleaching of its absorbance. Rather, the electrons rapidly relax to the ground state, with no concomitant change in the absorbance.

The same point may be demonstrated differently, by carrying out a two-pulse experiment on O_2-saturated solution containing 2−5 vol. % of glycerol (O_2 was used for photoreversibility, see section 2). As shown in section 3.1, addition of 5 vol. % glycerol causes ca. 45% decrease in the prompt TA signal from the trapped hole, due to rapid reaction with chemisorbed glycerol. Following the same trend, the ratio q_λ decreases by ca. 50% at $t_{21} = 25$ ns (Figure 11). At later delay times, there is a slow decay of the TA signal from the holes due to their reaction with glycerol (Figures 4b, 5b, and 9). The fraction q_λ plotted as a function of the delay time t_{21} tracks the hole scavenging (Figure 11). We conclude that the presence of a hole on the same TiO_2 nanoparticle is required for the decay of the photoexcited electron; in the absence of the hole, there is no decay. Conversely, any reaction that depletes the hole reduces the photobleaching efficiency.

We turn now to the quantum yield for the 532 and 1064 nm photobleaching. This quantity can be calculated from the known photobleaching fraction q_λ and the laser fluence, provided that the molar absorptivity of the species at the photoexcitation wavelength is known. Unfortunately, there is a large scatter in estimates for the molar absorptivity of trapped electrons in aqueous TiO_2 nanoparticles. Photochemical studies by Graetzel and co-workers suggested $\epsilon_{620} = 1200\ M^{-1}\ cm^{-1}$ in acidic[6] and $\epsilon_{780} = 800\ M^{-1}\ cm^{-1}$ in alkaline solutions.[26] Pulse radiolysis measurements of Safrany et al.[28] suggested $\epsilon_{800} = 700\ M^{-1}\ cm^{-1}$. Spectroelectrochemical measurements of Fitzmaurice and co-workers gave $\epsilon_{700} = 900-1000\ M^{-1}\ cm^{-1}$.[27] Using the absorption spectrum of the electron given by trace (iv) in Figure 2 and the estimate given by Safrany et al.,[28] the extinction coefficients for the electron at both 532 and 1064 nm are ca. 480 $M^{-1}\ cm^{-1}$, and the quantum yields for photobleaching are ca. 0.28 and 0.024, respectively.

4. Discussion

4.1. Synopsis. Here we briefly summarize our observations. The TA spectrum in the visible is composite. Two species contribute to this spectrum: (i) trapped electron, which has roughly the same absorption spectrum as the species generated by electron injection and reduction of TiO_2 nanoparticles and films (e.g., refs 26, 27, and 28), and (ii) trapped hole, which has an absorption spectrum in the visible range.[8−10,23] These two species decay by recombination that proceeds over many decades in time; the resulting spectrum does not evolve in time because both species simultaneously decay in the recombination event. When the electron is detrapped by 1064 or 532 nm photoexcitation, the resulting free, mobile electron rapidly recombines with the hole, and both species disappear from the TA spectrum. The quantum yield of the photobleaching by visible light is large, ca. 0.28 for 532 nm photoexcitation. When the hole is scavenged, photostimulated recombination is suppressed.

Recently, Beermann et al.[36] observed longer time-of-flight and decreased transferred charge when the photocurrent induced by 308 nm laser excitation of TiO_2 films was measured under continuous-wave irradiation by light with $\lambda > 420$ nm. The authors explained this behavior by "emptying of the initially filled traps by the visible light".[36] As suggested by our results, this "trap emptying" is followed by electron−hole recombination that depletes the charge flowing through the conductivity cell.

The light-absorbing hole can be selectively depleted by reaction with chemi- and physisorbed polyols,[7−9,25] such as glycerol. Most of this hole scavenging is very rapid (occurring in < 6 ns), and there are good reasons to believe that it involves a chemisorbed polyol molecule at the nanoparticle surface (see ref 25 for more discussion). This conclusion is in line with observations for hydroxylated aromatic molecules, which suggest that the predominant reaction route involves rapid, efficient electron transfer (most likely, involving the precursor of the trapped hole) to an adsorbed (most likely, chemisorbed via oxygen bridge) molecule.[25,37,38] However, for glycerol and other polyols,[25] this rapid scavenging is not 100% efficient, even at high polyol concentration. Approximately 45% of the holes survive this rapid process by descent into deep traps at the nanoparticle surface and slowly react with physisorbed glycerol molecules over the first 200 ns after the photoexcitation. There is also a small subset of light-absorbing holes (<10% of the total population) that are not scavenged by glycerol in either reaction; these are holes trapped in the nanoparticle interior (or, perhaps, the subsurface). Given the low concentration of electron−hole pairs generated in our experiments (1−2 pairs per nanoparticle), the depletion of the hole by a reaction with glycerol leaves an electron, which does not have a recombination partner on the same nanoparticle. Such electrons persist in solution for many tens of microseconds.

While these scenarios are consistent with our observations and find support in other studies, there is a troubling aspect to such an interpretation of the results. Namely, it is commonly believed that trapped holes in titania nanoparticles do not absorb light in the visible. Most researchers, following the original study by Rothenberger et al.,[6] assume that only *electrons* absorb in the visible, and this viewpoint has been supported by pulse radiolysis studies[39,40] in which the holes were shown to absorb at $\lambda < 400$ nm (section 4.3). Although there have been several studies, the results of which are contrary to the assumption that only electrons absorb in the visible,[8−10,23,30] it is prudent to consider alternative scenarios in which the hole does not absorb in the visible to explain our results.

4.2. Alternative Scenarios: Two-Electron Models. In this section we examine several scenarios in which the spectral transformations observed in section 3.1 are interpreted in terms of two or more light-absorbing electron species. In these scenarios, the hole is assumed to absorb in the UV,[39,40] outside of our observation range.

In the first class of such scenarios, surface modification of TiO_2 nanoparticles by glycerol results either in the formation of a new trapping site for the electron or elimination of a subset of such trapping sites. In particular, EPR studies[3] suggest that surface modification of TiO_2 nanoparticles results in the elimination and/or modification of electron traps at the nanoparticle surface.

The EPR studies of photoilluminated frozen solutions of titania nanoparticles demonstrate that, in the absence of the hole scavenger, most of the electrons in these nanoparticles recombine with the holes; the only species that survive are *interior* electrons. In the presence of hole scavengers, this recombination is inhibited and both the interior and surface of Ti^{III} centers (which have different degrees of *g*-tensor anisotropy) are observed by EPR spectroscopy.[3,15,18] In acidic solutions, most of the electrons are trapped at the surface of TiO_2 nanoparticles. These surface centers were not observed in TiO_2 nanoparticles whose surface is modified by chelating agents, such as cysteine.[3,17] Frequently, the surface modification results in the formation of new types of surface electron centers, with different EPR spectra.[3,17,18] Thus, a possible way to interpret our results is to assume that the TA spectrum observed in glycerol solutions (trace (i) in Figure 2) is from the interior electrons, whereas the spectrum in aqueous solutions without hole scavengers (trace (iii) in Figure 2) is a composite spectrum originating from both the interior and surface-trapped electrons.

First, we consider the possibility that the TA spectrum in the aqueous solution (without glycerol) is composite. If this were the case, two unlikely coincidences should occur, namely, (i) the decay kinetics for different electron species should be identical over many decades in time (as otherwise the TA spectrum would be time dependent), and (ii) the photobleaching of these species by 532 and 1064 nm light should be exactly the same (as otherwise selective photobleaching of one of these species would occur). The only way in which such a situation might occur naturally would involve rapid equilibrium involving these different electron species (that would have to occur well within the duration of the photoexcitation pulse). For some electron species (e.g., the conduction band electron and electrons in shallow traps), such a rapid equilibration is quite likely (section 4.5). To account for our data (assuming that the TA spectrum is from the electrons only) it is necessary to postulate that the TA spectrum observed in the aqueous solution is either from a *single* electron species or several such species in rapid equilibrium. The spectral transformation occurring in the glycerol solutions has to be interpreted as evidence that the modification of TiO_2 nanoparticles by glycerol leads to the formation of a new type of electron trap or, alternatively, to the elimination of certain surface traps, which shifts the equilibrium between the light-absorbing electron species contributing to the TA spectrum in the aqueous solution.

We turn, therefore, to the scenario, in which the modification of the TiO_2 surface by glycerol results in a new type of the electron trap.[3,17,18] The electrons descend into such traps in preference to the ordinary traps at the surface of a TiO_2 nanoparticle in the aqueous solution. To distinguish between the corresponding electron species, we will denote the electron in the regular trap as e_w^- and the electron in the polyol-modified trap as e_g^- . The "instantaneous" transformation of the TA spectrum in Figure 4b would be interpreted as evidence for the competition between these two traps for the conduction band electron. The spectral transformation observed in the first 200 ns would be indicative of the slow $e_w^- \rightarrow e_g^-$ transfer from the shallower to the deeper trap. In such a case, each intermediate spectrum in Figure 4b would be a weighted sum of the initial spectrum (trace (i)) from e_w^- and the final spectrum (trace (ii)) from e_g^- . This is indeed the case (section 3.1). While this interpretation would be consistent with our observations, it poses three problems. First, despite their different nature, e_w^- and e_g^- would be required to have *exactly* the same spectra for $\lambda > 900$ nm. Second, it seems unlikely that e_g^- (which is the electron in a *deeper* trap) has an absorption band to the red of e_w^- (which is the electron in a *shallower* trap). Third, absorption spectra similar to traces (ii) and (iv) in Figure 2 have been observed from reduced TiO_2 nanoparticles and films containing no

glycerol (e.g., refs 27 and 28). Thus, this scenario is unsatisfactory. [41]

We are left, therefore, with a scenario in which binding to glycerol eliminates a subset of surface traps and thereby shifts the equilibrium between the light-absorbing electron species, one of which has the absorption spectrum (mis)identified in section 3.1 as that from the trapped hole. There are data in the literature that seemingly support such a scenario.[42,43] For example, it has been observed that electrochemical reduction of thin anatase films in a certain range of potentials yields an electron species (see Figure 2 in ref 42) whose spectrum resembles the TA spectrum shown by trace (ii) in Figure 2. This scenario, however, also poses problems, because not only the prompt but also the "final" spectrum (attained at 200 ns) would depend on the glycerol concentration since the equilibrium between the electron species would depend on the availability of unmodified surface traps which, in turn, would depend on the extent of binding of these traps to glycerol. A related problem is how to explain the slow transformation of TA spectra in Figure 4b and the results of Figure 11. Since the postulated equilibrium between different electron species has to be rapid, the slow process can only involve transformations of the traps themselves while the electron resides in these traps. While it is possible to envision such transformations, their thermodynamics and kinetics would strongly depend on the structure of the surface modifier. Since exactly the same "final" spectrum is observed for all polyols and carbohydrates,[25] including poly(vinyl alcohol),[26] this scenario is also unsatisfactory. Last, it is difficult to account for the fact that spectra very similar to these "final" spectra have been observed from reduced hydrated TiO_2 containing no hole scavengers or surface modifiers.[27]

As seen from our examination, all scenarios involving elimination or modification of electron traps appear to run into one problem or another. There exists, however, a class of the two-electron scenarios that avoids these problems. Specifically, it may be postulated that the presence of the hole on the same nanoparticle modifies the absorption spectrum of the electron in the visible. In other words, the spectrum given by trace (iii) in Figure 2 is from a self-trapped exciton, whereas trace (i) originates from the decoupled electron that resides on a TiO_2 nanoparticle without the hole. The dispersive recombination of electron−hole pairs (Figure 1) is then viewed as the collapse of the exciton. As shown in Figure 7S, when the TA spectrum in water is plotted as a function of photon energy E_{ph}, the spectrum for $E_{ph} > 1.25$ eV is Gaussian, as would be expected for an exciton-like species. It is easy to see that all statements made in sections 3 and 4.1 can be restated in the exciton model by renaming the "light-absorbing hole" or "electron-hole" pair as "trapped exciton", because any process that depletes the hole automatically converts one kind of spectrum to another. In other words, our results appear to be equally compatible with the existence of a light-absorbing hole or a self-trapped exciton in aqueous TiO_2 nanoparticles. Below, we consider both of these possibilities in more detail.

4.3. Light-Absorbing Holes: Pro and Contra. A photogenerated hole absorbing light in the visible would account for our observations (sections 3 and 4.1). Such a rationale is not without a precedent, as there have been previous reports of such holes from photoexcited TiO_2 nanoparticles and films, both on the picosecond [30] and nanosecond time scales.[8−10,23] Perhaps, the strongest evidence of holes absorbing in the visible has been given by Bahnemann et al.,[8−10] who observed a TA spectrum from photoexcited aqueous TiO_2 nanoparticles impregnated with small islands of metallic platinum ("platinized" nanoparticles). The Pt patches rapidly remove photogenerated electrons from the TiO_2 nanoparticles, leaving behind the hole. The resulting species oxidizes Br^- to Br_2^- and has an absorption spectrum with an onset at 700−800 nm[10] and a maximum around 400 nm[8] or 470 nm.[10] This spectrum (Figure 5b) bears no resemblance to the spectra of "holes" generated in pulse radiolysis (see below). On the other hand, this spectrum is similar to the one shown in Figure 1, trace (ii) and Fig, 5b, trace (i).

Recently, Yoshihara et al.[23] reported observations of wide-range TA spectra (0.4−2.5 μm) of photoexcited TiO_2 nanocrystalline films in contact with liquid D_2O and CD_3OD. The methanol was used to scavenge the holes in less than 10 ns. Similarly to our results (section 3.1), the presence of the hole scavenger made no difference in the TA spectra in the near-IR (in this case, for $\lambda > 1.6$ μm), suggesting that the TA signal originated from electrons only. By comparison of the suitably normalized TA spectra (as done in section 3.1), the spectrum of the tentative hole was obtained (see Figure 6 in ref 23). Except for a small extension to the red of 1 μm, this spectrum closely resembles the one shown by trace (ii) in Figure 2.

Despite these observations, the general consensus is in favor of a UV-absorbing hole. Two arguments supporting this may be given. First, the reaction of TiO_2 nanoparticles with strong oxidizing radicals, such as radiolytically generated $SO_4^{\bullet-}$ and $HO^\bullet$ radicals, yields a species that absorbs in the UV, with an onset below 400 nm.[39,40] Assuming that these radicals react with the nanoparticles by electron transfer, it may be inferred that the holes do not absorb in the visible. To account for the TA spectrum of the tentative holes observed by Bahnemann et al.,[8,9] Lawless et al.[39] suggested that this spectrum originated from the photoexcitation of Pt islands rather than TiO_2 nanoparticles themselves. This argument does not seem to be supported by the results of the present study (or by the results in refs 23 and 30), in which the absorbance in the visible similar to that reported by Bahnemann et al.[8−10] was observed in the absence of platinum. We may further object that the pulse radiolysis studies do not provide decisive evidence that electron transfer between these radicals and the TiO_2 nanoparticle indeed occurs (as also noted by Lawless et al.).[39] The occurrence of the electron transfer, with a nearly diffusion controlled rate,[39,40] seems unlikely as, according to Rajh et al.,[40] the standard potentials for the sulfate and hydroxyl radicals (2.4 and 1.9 V, respectively, vs normal hydrogen electrode, NHE) are less positive than this potential for the valence band hole in hydrated anatase (2.85 V vs NHE, at pH = 3).

It is possible that the reaction of hydroxyl radical with a TiO_2 nanoparticle yields $HO^\bullet_{ads}$ as the main product (the same applies to the $SO_4^{\bullet-}$ radical). As mentioned in the Introduction, it is presently believed that at least two hole species, the mobile hole (observed in our TA experiments) and $HO^\bullet_{ads}$, are generated by UV photolysis of aqueous TiO_2 nanoparticles.[19−21] The latter species is a minor product with a quantum yield ca. 100 times lower than that of the more abundant mobile hole.[19] Pulse radiolysis data alone are insufficient to determine which reaction, surface addition or electron transfer, occurs when these radicals encounter a nanoparticle in the water bulk. A convincing demonstration of the occurrence of electron transfer would be the similarity of reaction patterns and rates for radiolytically and photolytically generated holes. Such a demonstration is presently lacking, and this absence of supportive results weakens the whole argument favoring the UV-absorbing holes.

Second, the O *2*p radicals of the $Ti^{IV}-O^\bullet$ type identified by EPR[3,18] as possible hole centers are not expected to be strong

absorbers in the visible. The obvious objection to this argument is that the light-absorbing hole might be a different type of oxygen hole center. In particular, if the hole were trapped on the bridging oxygen of a $Ti^{IV}-O-M^{n+}$ center, where M^{n+} is the (impurity) metal cation, the crystal field of this cation would split the degenerate O 2p orbitals, resulting in the absorption of visible light by the hole center.[44] A classical example of such an impurity center is the aluminum hole center in smoky quartz (SiO_2/Al). In this solid, overcoordinated Al^{III} ion substitutes for Si^{IV}, providing a negatively charged trap for the hole. While the $Si^{IV}-O^{\bullet}$ center does not absorb visible light, $Si^{IV}-O^{\bullet}\cdots Al^{III}$ centers strongly absorb across the visible.[44] Note that an impurity content of just 7 ppm would be sufficient to have one metal ion per TiO_2 nanoparticle in our photosystem (if all such ions are in the TiO_2 phase). The typical concentrations of impurity ions in our colloidal solutions were much higher (> 40 ppm). Thus, a commonly occurring bi- or trivalent impurity ion, such as Al^{III}, might be the sought-after progenitor of the oxygen hole center. Since such an ion would substitute for tetravalent Ti^{IV}, the precursor of the hole would be a negatively charged trap. Such a trap can be a deeper trap than $Ti^{IV}-O^{-}$ or $Ti^{IV}-OH$ groups at the surface that are believed to be the precursors of the $Ti^{IV}-O^{\bullet}$ hole. If this impurity ion is diamagnetic and has small nuclear dipole moment, no additional fine or hyperfine structure would be observed in the EPR spectra of the resulting hole center. Given the high crystallinity of anatase nanoparticles,[2,32] it is likely that such an impurity ion would be at or near the nanoparticle surface. Since the partition of (impurity) ions between the aqueous and TiO_2 phases would be pH dependent, sensitivity of the TA spectrum to pH of the solution[26] finds a natural explanation. (There is also an interesting possibility that an undercoordinated titanium atom at the surface plays the role of the "impurity" cation).

While our identification of photogenerated holes with impurity-related oxygen hole centers is tentative, this suggestion may be verified without going to the extreme effort of eliminating the ubiquitous impurity. The unpaired electron on the oxygen would be coupled to the nucleus of the impurity ion by weak dipole interaction. Such an interaction may be observed using electron spin−echo envelope modulation (ESEEM) and electron nuclear double resonance (ENDOR) spectroscopies.

In the review of this paper, a question was raised as to why the spectrum of the hole persists over tens of microseconds, whereas it is believed that the "hole" reacts with water or OH^{-} groups at the nanoparticle surface, yielding $HO^{\bullet}_{ads}$ and, consequently, free hydroxyl radicals. There is abundant literature documenting the formation of free hydroxyl radicals in photolysis of TiO_2,[16,19−21] which can be detected, for example, via its reactions with nitroxide spin traps and nitroxyl radicals.[16] It should be stressed that even if these hydroxyl radicals were produced via a reaction of trapped holes with water, the conversion would be too low to be observed in our experiments, because the overall quantum yield of free hydroxyl radicals, as determined using spin trapping techniques, is just $10^{-4}-10^{-3}$.[16b] Furthermore, it is usually assumed that the hole species reacting with water or OH^{-} groups is a short-lived energetic *precursor* of the surface-trapped hole. The product analysis and spin trapping studies do not indicate whether the hydroxyl radicals are formed promptly or gradually. While there are data in the literature suggesting gradual release of the hydroxyl radicals from trapped "holes" on aqueous TiO_2 nanoparticles (e.g., ref 37), in our opinion, such results may also be explained by addition and/or abstraction reactions of $Ti^{IV}-O^{\bullet}$ species followed by hydrolysis of the Ti−O bond or even by slow desorption of the $HO^{\bullet}_{ads}$ radical itself.

4.4. Self-Trapped Exciton. As discussed in section 4.2, the alternative explanation of our results would be admitting that the holes in the aqueous TiO_2 nanoparticles do not absorb in the visible, and the vis spectrum shown in Figure 2, trace (iii) is from a self-trapped exciton. We are aware of no evidence for the existence of such excitons in aqueous TiO_2 nanoparticles, although there is ample evidence that self-trapped excitons are formed in crystalline anatase[45] and TiO_2 films.[46] In these materials, self-trapped excitons decay by radiative recombination and yield photoluminescence spectra centered at 2.4 eV.

The chief problem is to explain the *absorption* spectrum of the tentative exciton. The exciton in crystalline and thin-film anatase contributes to the smooth Urbach tail at the band edge;[45] these excitons do not yield the absorption spectrum shown in Figure 2, trace (iii). Furthermore, one would expect that strong electron−hole coupling would be readily identifiable in the EPR spectra of UV illuminated TiO_2 nanoparticles. No evidence for such a coupling has been found. Thus, the self-trapped exciton scenario, while plausible, lacks experimental support.

4.5. Photostimulated Electron Detrapping. The very fact that photoexcitation of electrons results in their rapid recombination with trapped holes suggests their identity as *trapped* charges. A claim is sometimes found in the literature that the 700−900 nm band of the trapped electron is actually from free conduction band (CB) electrons. It is difficult to explain how such a free carrier could have existed on the same TiO_2 nanoparticle with the hole over many microseconds, to give the composite spectrum shown in Figure 2, trace (iii). The view that absorbance in the visible and near-IR originates from free CB electrons appears to be inconsistent with many observations. The problem is that, with most techniques, it is difficult to distinguish between the "free" carriers and band-tail charges in shallow traps (from which thermal emission of the free carriers can readily occur). The preceding does not mean that metastable CB electrons cannot occur in TiO_2 under favorable conditions (e.g., such species were observed in the diffuse reflectance IR spectra of heat- and oxygen-treated, UV-illuminated hydrated rutile surfaces); [47] the point is that such long-lived species do not occur in aqueous TiO_2 nanoparticles.

CB electrons injected from dye molecules chemisorbed at the surface of nanocrystalline TiO_2 films can be observed for >1 ns, using time-resolved infrared (IR)[14] and terahertz (THz)[48] spectroscopies. Recent results of Turner et al. [48] suggest that these CB electrons exhibit features that are more consistent with Anderson localization and transport by thermally activated hopping. The THz conductivity is dominated by backscattering, and the electrons have strikingly non-Drude behavior. "Hot" electrons observed in the first 330 fs after the electron injection are more Drude-like,[48] and only such species can be regarded as "free" CB electrons.

Following the rapid trapping of free carriers by traps in the TiO_2 nanoparticles (<200 fs,[4] <330 fs[48]), the mobility of the electron is orders of magnitude lower[22,49] than the drift and Hall mobilities of CB electrons in high-quality anatase films.[50] From the extensive data on microwave (GHz) photoconductivity obtained by Warman and co-workers[22,49] and Martin et al.,[51] it appears that the charge migration in these nanoparticles (typical mobilities are 5×10^{-4} cm^2/Vs for holes and $10^{-3}-10^{-1}$ cm^2/Vs for electrons, depending on the sample)[22,49] is facilitated either by small polaron hopping or by thermal emission of free carriers from shallow traps.[22] The depth of the traps has been estimated by different authors as being from 60 to 100 meV[43,51]

to 400−600 meV[36,42] (the higher estimates seem to be incompatible with the thermal emission mechanism mentioned above). Many types of electron traps coexist in the aqueous nanoparticles, and the scatter in the estimates reflects the fact that different electron populations are observed in different experiments.

The shallow-trap electrons would readily account for the diffuse IR absorbances observed in refs 12, 23, and 47. Indeed, with a few exceptions[52] all observations of persistent "free electrons" in titania nanoparticles can be interpreted as evidence for the existence of such shallow-trap electrons. As considerable delocalization of the electron wave function is likely in these shallow-trap states, evidence for such a delocalization (e.g., the recent observation of Stark effect on the Ti−OH vibrations)[53] does not necessarily indicate the involvement of the free electron. In any case, this observation is incompatible with the view that the "free CB electrons" are restricted exclusively to the nanoparticle interior.

In this regard, it is noteworthy that the quantum yield for electron photobleaching decreases by an order of magnitude from 532 nm (2.33 eV) photoexcitation to 1064 nm (1.17 eV) photoexcitation (section 3.2). Only electrons in deep traps (0.5−1 eV) would account for such a precipitous decrease in the photobleaching efficiency. The highly asymmetrical shape of the electron spectrum (trace (i) in Figure 7S) also suggests that this spectrum is composite. Specifically, it appears that a broad absorption line centered at ca. 1.5 eV is juxtaposed on a diffuse absorbance that increases as $\lambda^{1.5-2}$ toward the red (this absorbance may be the blue extension of the IR spectra observed by Hoffmann et al. from oxygen-treated photoilluminated rutile TiO_2 surfaces).[47] Our spectral data hint that at some point, as the wavelength of the analyzing light increases toward the IR, there should be a gradual transition from a TA spectrum dominated by electrons residing in deep traps (which add little to the dc and ac conductivity) to a TA spectrum dominated by electrons in shallow traps (responsible for the electron conduction). For TiO_2 nanoparticles in aqueous solutions, such a transition occurs somewhere in the mid-IR (perhaps, around 1.5−1.6 μm),[23] where the electron absorption in aqueous TiO_2 nanoparticles cannot be observed due to the strong absorption of the IR light by the solvent. Very clear separation of these two spectral contributions in the 0.4−2.5 μm range has been recently demonstrated by Yoshihara et al.[23] for photoexcited, thin TiO_2 nanocrystalline films wetted by D_2O and CD_3OD. It is apparent from their results that the electron spectrum is composed of a bell-shaped absorbance in the visible (centered at ca. 770 nm) riding on top of a diffuse absorbance of shallow-trap electrons that increases as $\lambda^{1.7}$ toward the IR.[23] The two components contribute equally at 900 nm. Yoshihara et al.[23] place the onset of the vis-band absorbance at 1.2 μm, which would explain the low quantum efficiency of electron photobleaching induced by the absorption 1064 nm light (section 3.2).

These two spectral contributions correspond to the electrons in deep and shallow traps, respectively (Yoshihara et al.,[23] though, attribute the diffuse component to the free CB electron). Lisachenko et al.[54] observed the same two spectral contributions in diffuse reflectance spectra of dry TiO_2 powders reduced by H_2 and CO. In addition, they observed weak absorption bands at 2.5 and 2.8 eV attributed to electrons trapped at oxygen vacancies. Conceivably, these may be the deep-trap species identified in the recent spetroelectrochemical studies of Beermann et al.[36] As discussed in section 4.2, a composite nature of the electron absorbance would be compatible with the observations on the nanosecond time scale, provided that the equilibration of trapped states absorbing in the visible and near-IR occurs on a much shorter time scale. Otherwise, it is impossible to account for the lack of selective bleaching of different electron species (sections 3.2 and 4.2). Unfortunately, the existing picosecond data for uncoated TiO_2 nanoparticles are limited to a narrow spectral interval between 400 and 700 nm where both the electron and hole absorb probe light (section 3.1). While there is considerable spectral evolution within the first 50−100 ps,[4,30,31] this evolution can be interpreted in many different ways.

It is worth mentioning that there are results in the literature that appear to contradict the notion that different trapped-electron species on the same TiO_2 nanoparticle rapidly equilibrate. Recently, Dimitrijevic et al.[32] used pulse radiolysis to study the reaction of TiO_2 nanoparticles with hydrated electrons. The resulting TA spectra did not look like the spectra from "persistent" electrons obtained by Safrany et al.[28] using the same method for similar nanoparticles. The electron absorbance for $\lambda = 1.2-2$ μm was flat;[32] there was also a bell-shaped absorption band with a maximum at 680 nm. Full coverage of the nanoparticle by dopamine selectively removed that bell-shaped band, leaving a spectrum that was flat over the entire visible and near-IR. One would expect that the absorption spectrum of the "electron" does not depend on the method used for its generation, be it photolysis, pulse radiolysis, or electrochemical reduction. While it is possible that different electron species are generated in photolysis and radiolysis, the postulated rapid equilibration would eliminate any such differences. Yoshihara et al.[23] reported selective (though partial) scavenging of the vis-absorbing electrons in oxygen-saturated CD_3OD solutions. There were previous reports of rapid modification of the TA spectrum of the electron by oxygen.[6,10] We did not observe any such effect in our studies, and the results of Gao et al.[34] suggest a very low rate for the reaction of oxygen with electrons in TiO_2 nanoparticles. Again, any evidence of the selective scavenging would indicate that there is a subset of trapped electrons that is not involved in the rapid equilibrium with other states. As explained in sections 3.2 and 4.2, coexistence of several distinctive light-absorbing electron species on the same nanoparticle, in the absence of the rapid equilibration, is not supported by our results.

5. Conclusions

It is shown that 532 and 1064 nm laser photoexcitation of trapped electrons generated in 355 nm photolysis of aqueous titania (TiO_2) nanoparticles (diameter 4.6 ± 0.5 nm, pH = 4) causes rapid photobleaching of their absorbance band in the visible and near-IR. This photobleaching occurs within the duration of the laser pulse (6 ns fwhm); it is caused by photoinduced electron detrapping followed by recombination of the resulting free electron and a trapped hole. The quantum yield for the electron photobleaching is ca. 0.28 for 532 nm and ca. 0.024 for 1064 nm photoexcitation. The drastic reduction in the quantum efficiency with increasing wavelength of the photoexcitation light suggests that the absorption spectrum of the electron in the near-IR originates both from the electrons in shallow traps and the electrons in deep traps; there should be rapid (<1 ns) equilibration between all such states.

Complete separation of the spectral contributions from trapped electrons and holes is demonstrated using glycerol as a selective hole scavenger (Figure 2). The holes absorb across the entire visible; their absorption increases toward the UV. The electron absorption increases toward 900−1000 nm and then slowly decreases toward the IR. The characteristic 650 nm band of

photoilluminated aqueous TiO_2 nanoparticles is composite. Our results (as well as the results of Bahnemann et al.)[8−10] and Yoshihara et al.[23] indirectly suggest that holes obtained by reaction of oxidizing radicals (such as hydroxyl) with TiO_2 nanoparticles[39,40] have absorption properties different from those of the photogenerated holes. We speculate that the vis-light absorbing O 2p holes originate from a common ion impurity in colloidal TiO_2. This suggestion can be verified using advanced magnetic resonance spectroscopies.

In the absence of the hole scavenger (glycerol), no evolution of the transient absorbance spectra (400 to 1350 nm) was observed out to 10 μs, both in N_2- and O_2-saturated aqueous solutions. In the presence of 5 vol. % glycerol, ca. 45−50% of the light-absorbing holes are scavenged promptly within the duration of the 355 nm photoexcitation pulse, another 40−45% of the holes are scavenged at a slower rate over the first 200 ns after the photoexcitation pulse, and the remaining 5−10% are not scavenged, even at the high concentration of the scavenger (>10 vol. %). A reaction with chemi- and physisorbed glycerol can account for the prompt and the slow hole decays, respectively. The mechanism for this reaction is further discussed in the companion paper.[25] Rapid trapping of the mobile hole by chemisorbed aromatic molecules with anchoring −OH and −COOH groups has been postulated by Majima and coworkers[38] and Goldstein et al.[37] among others; our results for polyols are supportive of the general mechanism suggested in these studies.

Our results can also be explained by a mechanism in which the absorption spectra of electrons with and without the hole present on the same TiO_2 nanoparticle are different (sections 4.2 and 4.4). This interpretation can be construed as evidence for the formation of self-trapped excitons in the anatase nanoparticles. However, at the present time this explanation has little experimental support. Other scenarios in which the composite spectrum shown in Figure 2 originates from two or more electron species (rather than the electron and the hole) also seem to be excluded by our results (section 4.2).

Acknowledgment. I.A.S. thanks Drs. T. Rajh, P. V. Kamat, D. Meisel, and J. Rabani for stimulating discussions and Drs. N. Dimitrijevic and Z. V. Saponjic for the preparation of some TiO_2 samples. This work was performed under the auspices of the Office of Science, Division of Chemical Science, US-DOE under contract number W-31-109-ENG-38.

Supporting Information Available: A single PDF file containing Figures 1S to 7S with captions. This material is available free of charge via the Internet at http://pubs.acs.org.

References and Notes

(1) For comprehensive reviews, see, for example, Henglein, A. *Pure Appl. Chem.* **1984**, *56*, 1215. Hoffmann, M. R.; Martin, S. T.; Choi, W.; Bahnemann, D. W. *Chem. Rev.* **1995**, *95*, 69. Linsebigler, A. L.; Lu, G.; Yates, J. T., Jr. *Chem. Rev.* **1995**, *95*, 735. Tryk, D. A.; Fujisima, A.; Honda, K. *Electrochem. Acta* **2000**, *45*, 2363. Kamat, P. V. *J. Phys. Chem. B* **2002**, *106*, 7729.

(2) Rajh, T.; Chen, L. X.; Lukas, K.; Liu, T.; Thurnauer, M. C.; Tiede, D. M. *J. Phys. Chem. B* **2002**, *106*, 10543. Chen, L. X.; Rajh, T.; Jager, W.; Nedeljkovic, J.; Thurnauer, M. C. *J. Synchrotron Radiat.* **1999**, *6*, 445.

(3) Rajh, T.; Poluektov, O. G.; Thurnauer, M. C. In *Chemical Physics of Nano-structured Semiconductors*; Kokorin, A. I., Ed.; NOVA Science Publ., Inc.: New York, 2003; p 1.

(4) Cavalieri, J. J.; Colombo, D. P., Jr.; Bowman, R. M. *J. Phys. Chem. B* **1998**, *102*, 1341. Colombo, D. P., Jr.; Bowman, R. M. *J. Phys. Chem.* **1996**, *100*, 18445. Colombo, D. P., Jr.; Roussel, K. A.; Saeh, J.; Skinner, D. E.; Cavalieri, J. J.; Bowman, R. M. *Chem. Phys. Lett.* **1995**, *232*, 207. Colombo, D. P., Jr.; Bowman, R. M. *J. Phys. Chem.* **1995**, *99*, 11752. Skinner, D. E.; Colombo, D. P., Jr.; Cavalieri, J. J.; Bowman, R. M. *J. Phys. Chem.* **1995**, *99*, 7853.

(5) Serpone, N.; Lawless, D.; Khairutdinov, R.; Pelizzetti, E. *J. Phys. Chem.* **1995**, *99*, 16655.

(6) Rothenberger, G.; Moser, J.; Graetzel, M.; Serpone, N.; Sharma, D. K. *J. Am. Chem. Soc.* **1985**, *107*, 8054.

(7) Henglein, A. *Ber. Bunsen-Ges. Phys. Chem.* **1982**, *86*, 241.

(8) Bahnemann, D.; Henglein, A.; Spanhel, L. *Faraday Discuss Chem. Soc.* **1984**, *78*, 151.

(9) Bahnemann, D.; Henglein, A.; Lilie, J.; Spanhel, L. *J. Phys. Chem.* **1984**, *88*, 709.

(10) Bahnemann, D. W.; Hilgendorff, M.; Memming, R. *J. Phys. Chem. B* **1997**, *101*, 4265.

(11) Duonghong, D.; Ramsden, J.; Graetzel, M. *J. Am. Chem. Soc.* **1982**, *104*, 2977.

(12) Yamakata, A.; Ishibashi, T.; Onishi, H. *Chem. Phys. Lett.* **2001**, *333*, 271.

(13) Grela, M. A.; Colussi, A. J. *J. Phys. Chem.* **1996**, *100*, 18214.

(14) Ellingson, R. J.; Asbury, J. B.; Ferrere, S.; Ghosh, H. N.; Sprague, J. R.; Lian, T.; Nozik, A. J. *J. Phys. Chem. B* **1998**, *102*, 6455. Ghosh, H. N.; Asbury, J. B.; Weng, Y.; Lian, T. *J. Phys. Chem. B* **1998**, *102*, 10208. Ghosh, H. N.; Asbury, J. B.; Lian, T. *J. Phys. Chem. B* **1998**, *102*, 6428. Asbury, J. B.; Ellingson, R. J.; Ghosh, H. N.; Ferrere, S.; Nozik, A. J.; Lian, T. *J. Phys. Chem. B* **1999**, *103*, 3110. Wang, Y.; Asbury, J. B.; Lian, T. *J. Phys. Chem. A* **2000**, *104*, 4291. Weng, Y.-X.; Wang, Y.-Q.; Ashbury, J. B.; Ghosh, H. N.; Lian, T. *J. Phys. Chem. B* **2000**, *104*, 93. Asbury, J. B.; Wang, Y.-Q.; Hao, E.; Ghosh, H. N.; Lian, T. *Res. Chem. Internmed.* **2001**, *27*, 393. Asbury, J. B.; Hao, E.; Wang, Y.; Ghosh, H. N.; Lian, T. *J. Phys. Chem. B* **2001**, *105*, 4545.

(15) Howe, R. F.; Graetzel, M. *J. Phys. Chem.* **1985**, *89*, 4495. Howe, R. F.; Graetzel, M. *J. Phys. Chem.* **1987**, *91*, 3906. Moser, J.; Graetzel, M.; Gallay, R. *Helv. Chem. Acta* **1987**, *70*, 1596.

(16) (a) Jaeger, C. D.; Bard, A. J. *J. Phys. Chem.* **1979**, *83*, 3146. Riegel, G.; Bolton, J. R. *J. Phys. Chem.* **1995**, *99*, 4215. (b) Nosaka, Y.; Komori, S.; Yawata, K.; Hirakawa, T.; Nosaka, A. Y. *Phys. Chem. Chem. Phys.* **2003**, *5*, 4731 and references therein.

(17) Rajh, T.; Nedeljkovic, J. M.; L. X. Chen, O. P.; Thurnauer, M. C. *J. Phys. Chem. B* **1999**, *103*, 3515. Dubinski, A. A.; Perekhotsev, G. D.; Poluektov, O. G.; Rajh, T.; Thurnauer, M. C. *J. Phys. Chem. B* **2002**, *106*, 938.

(18) Micic, O. I.; Zhang, Y.; Cromack, K. R.; Trifunac, A. D.; Thurnauer, M. C. *J. Phys. Chem.* **1993**, *97*, 7277 and 13284.

(19) Ishibashi, K.; Fujishima, A.; Watanabe, T.; Hashimoto, K. *J. Photochem. Photobiol. A* **2000**, *134*, 139. See also Nosaka, Y.; S. Komori; Yawata, K.; Hirakawa, T.; Nosaka, A. *Phys. Chem. Chem. Phys.* **2003**, *5*, 4731.

(20) Gao, R.; Stark, J.; Bahnemann, D. W.; Rabani, J. *J. Photochem. Photobiol. A* **2002**, *148*, 387. See also Sun, L.; Bolton, J. R. *J. Phys. Chem.* **1996**, *100*, 4127.

(21) Rabani, J.; Yamashita, K.; Ushida, K.; Stark, J.; Kira, A. *J. Phys. Chem. B* **1998**, *102*, 1689.

(22) Warman, J. M.; de Haas, M. P.; Pichat, P.; Koster, T. P. M.; van der Zouwen-Assink, E. A.; Mackor, A.; Cooper, R. *Radiat. Phys. Chem.* **1991**, *37*, 433.

(23) Yoshihara, T.; Katoh, R.; Furube, A.; Tamaki, Y.; Murai, M.; Hara, K.; Murata, S.; Arakawa, H.; Tachiya, M. *J. Phys. Chem.* B **2004**, *108*, 3817.

(24) Yamakata, A.; Ishibashi, T.; Onishi, H. *J. Phys. Chem. B* **2002**, *106*, 9122. Yamakata, A.; Ishibashi, T.; Onishi, H. *Chem. Phys. Lett.* **2003**, *376*, 576.

(25) Shkrob, I. A.; Sauer, M. C., Jr.; Gosztola, D. *J. Phys. Chem. B* **2004**, *108*, 12512.

(26) Koelle, U.; Moser, J.; Graetzel, M. *Inorg. Chem.* **1985**, *24*, 2253.

(27) Boschloo, G.; Fitzmaurice, D. *J. Phys. Chem. B* **1999**, *103*, 7860. Enright, B.; Fitzmaurice, D. *J. Phys. Chem.* **1996**, *100*, 1027. O'Regan, B.; Graetzel, M.; Fitzmaurice, D. *Chem. Phys. Lett.* **1991**, *183*, 89. Redmond, G.; Fitzmaurice, D.; Graetzel, M. *J. Phys. Chem.* **1993**, *97*, 6951. Rothenberger, G.; Fitzmaurice, D.; Graetzel, M. *J. Phys. Chem.* **1992**, *96*, 5983.

(28) Safrany, A.; Gao, R.; Rabani, J. *J. Phys. Chem. B* **2000**, *104*, 5848.

(29) Kamat, P. V.; Bedja, I.; Hotchandani. *J. Phys. Chem. B* **1994**, *98*, 9137. Kormann, C.; Bahnemann, D. W.; Hoffmann, M. R. *J. Phys. Chem.* **1988**, *92*, 5196.

(30) Furube, A.; Asahi, T.; Masuhara, H.; Yamashita, H.; Anpo, M. *J. Phys. Chem.* **1999**, *103*, 3120.

(31) Arbour, C.; Sharma, D. K.; Langford, C. H. *J. Phys. Chem.* **1990**, *94*, 331.

(32) Dimitrijevic, N. M.; Saponjic, Z. V.; Bartels, D. M.; Thurnauer, M. C.; Tiede, D. M.; Rajh, T. *J. Phys. Chem. B* **2003**, *107*, 7368.

(33) Cline, J. A.; Jonah, C. D.; Bartels, D. M. *Rev. Sci. Instrum.* **2002**, *73*, 3909.

(34) Gao, R.; Safrany, A.; Rabani, J. *Radiat. Phys. Chem.* **2003**, *67*, 25.

(35) Such a conclusion is in accord with several other kinetic studies, suggesting that hole scavenging by chemisorbed molecules occurs on picosecond or femtosecond time scale (e.g., refs 4 and 14).

(36) Beermann, N.; Boschloo, G.; Hagfeldt, A. *J. Photochem. Photobiol. A* **2002**, *152*, 213.

(37) Goldstein, S.; Czapski, G.; Rabani, J. *J. Phys. Chem.* **1994**, *98*, 6586.

(38) Tachikawa, T.; Tojo, S.; Fujitsuka; Majima, T. *J. Phys. Chem. B* **2004**, *108*, 5859. *Langmuir* **2004**, *20*, 2753. Tojo, S.; Tachikawa, T.; Fujitsuka; Majima, T. *Phys. Chem. Chem. Phys.* **2004**, *6*, 960.

(39) Lawless, D.; Serpone, N.; Meisel, D. *J. Phys. Chem.* **1991**, *95*, 5166.

(40) Rajh, T.; Saponjic, Z. V.; Micic, O. I. *Langmuir* **1992**, *8*, 1265.

(41) A modification of the latter scenario, suggested to us by T. Rajh, is rapid injection of the electron from a ketyl radical (formed by oxidation of polyol) followed by the formation of a new type of trapped electron (for methanol, this process was observed by low-temperature EPR, see refs 3 and 18). Such a scenario seems unlikely given the low rate constants for this electron-injection reaction in the water bulk (where such reactions occur on the millisecond time scale; see ref 32 and Gao, R.; Safrany, A.; Rabani, J. *Radiat. Phys. Chem.* **2002**, *65*, 599). Even if the radical anchored at the nanoparticle surface reacted faster (and the formation dynamics of IR absorbance from the C═O group on rutile surface covered by 2-propanol studied in ref 24 suggest otherwise, indicating a half-life >50 μs), this scenario would present the same difficulty as the scenarios considered above.

(42) Boschloo, G.; Fitzmaurice, D. *J. Phys. Chem. B.* **1999**, *103*, 2228. See also Haque, S. A.; Tachibana, Y.; Klug, D. R.; Durrant, J. R. *J. Phys. Chem. B* **1998**, *102*, 1745. Boschloo, G. K.; Goossens, A. *J. Phys. Chem.* **1996**, *100*, 19489.

(43) Durrant, J. R. *J. Photochem. Photobiol. A* **2002**, *148*, 5.

(44) Griscom, D. L. In *The physics of SiO_2 and its interfaces*; Pantelides, S. T., Ed.; Pergamon Press: New York, 1978; p 232.

(45) Tang, H.; Lévy, F. J.; Berger, H.; Schmid, P. E. *Phys. Rev. B* **1995**, *52*, 7771.

(46) Tang, H.; Pasad, K.; Sanjines, R.; Schmid, P. E.; Lévy, F. J. *Appl. Phys.* **1994**, *75*, 2042.

(47) Szczepankiewicz, S. H.; Colussi, A. J.; Hoffmann, M. R. *J. Phys. Chem. B* **2000**, *104*, 9842. Szczepankiewicz, S. H.; Moss, J. A.; Hoffmann, M. R. *J. Phys. Chem. B* **2002**, *106*, 2922.

(48) Turner, G. M.; Beard, M. C.; Schmuttenmaer, C. A. *J. Phys. Chem. B* **2002**, *106*, 11716.

(49) Savenije, T. J.; de Hass, M. P.; Warman, J. M. *Z. Phys. Chem.* **1999**, *212*, 201. Warman, J. M.; de Haas, M. P.; Pichat, P.; Serpone, N. *J. Phys. Chem.* **1991**, *95*, 8858. Kroeze, J. A.; Savenije, T. J.; Warman, J. M. *J. Am. Chem. Soc.* **2004**, *126*, 7608−7618.

(50) Breckenridge, R. G.; Hosler, W. R. *Phys. Rev.* **1953**, *91*, 793. Frederikse, H. P. R. *J. Appl. Phys.* **1961**, *32*, 2211. Forro, L.; Chauvet, O.; Emin, D.; Zuppiroli, L.; Berger, H.; Lévy, F. *J. Appl. Phys.* **1994**, *75*, 633. See also ref 49.

(51) Martin, S. T.; Herrmann, H.; Hoffmann, M. R. *J. Chem. Soc., Faraday Trans.* **1994**, *90*, 3315 and 3323.

(52) The strongest argument in favor of the persistent vis-absorbing "free" electron that we found is that the absorbance keeps increasing linearly with the number of injected electrons per TiO_2 nanoparticle even when the density reaches 100 electrons/nanoparticle (ref 28), whereas the density of the electron-trapping sites is <15 traps/particle (ref 42 of this paper). In our view, this observation suggests little more than that the latter estimate is incorrect. The impedance studies of rutile *single crystals* suggest surface densities that are an order of magnitude larger; the trap density for a TiO_2 nanoparticle could only be higher.

(53) Szczepankiewicz, S. H.; Moss, J. A.; Hoffmann, M. R. *J. Phys. Chem. B* **2002**, *106*, 7654.

(54) Lisachenko, A. A.; Kuznetsov, V. N.; Zakharov, M. N.; Mikhailov, R. V. *Kinet. Catal.* **2004**, *45*, 189 and references therein.